https://doi.org/10.5194/nhess-2019-304
Preprint. Discussion started: 15 October 2019

Natural Hazards and Earth System Sciences
Discussions

Hydrogeomorphological analysis and modelling for a comprehensive understanding of flash-flood damaging processes: The 9th October 2018 event in North-eastern Mallorca

Joan Estrany[1,2*], Maurici Ruiz-Pérez[1,2,3], Raphael Mutzner[4], Josep Fortesa[1,2], Beatriz Nácher-Rodríguez[5], Miquel Tomàs-Burguera[6], Julián García-Comendador[1,2], Xavier Peña[4], Adolfo Calvo-Cases[7], Francisco J. Vallés-Morán[5]

[1]Mediterranean Ecogeomorphological and Hydrological Connectivity Research Team (http://medhycon.uib.cat), Department of Geography, University of the Balearic Islands, Carretera de Valldemossa Km 7.5, 07122 Palma, Balearic Islands, Spain
[2]Institute of Agro-Environmental and Water Economy Research –INAGEA, University of the Balearic Islands, Carretera de Valldemossa Km 7.5, 07122, Palma, Balearic Islands, Spain
[3]Service of GIS and Remote Sensing, University of the Balearic Islands, 07122 Palma, Balearic Islands, Spain
[4]Hydrique Engineers (http://www.hydrique.ch), Le Mont sur Lausanne, Vaud 1052, Switzerland
[5]Universitat Politècnica de València, Camí de Vera, s/n, València, 46022, Spain
[6]Estación Experimental de Aula Dei (EEAD-CSIC), Avenida Montañana, 1005, 50059 Zaragoza, Spain
[7]Inter-University Institute for Local Development (IIDL) Department of Geography, University of Valencia, Av. Blasco Ibáñez 28, 46010, Valencia, Spain

Correspondence to: Joan Estrany (joan.estrany@uib.cat)

Abstract. A flash-flood event hit in the 9th October 2018 the northeastern part of Mallorca Island, causing 13 casualties. This island is prone to catastrophic flash floods acting on a scenario that illustrates the deep landscape transformation of Mediterranean tourist resorts. As global change may exacerbate devastating flash floods, comprehensive analyses of catastrophic events are crucial to support effective prevention and mitigation measures. Field-based, remote-sense and modelling techniques were used in this study to evaluate rainfall-runoff processes at catchment scale linked to hydrological modelling. Continuous streamflow monitoring data revealed a peak discharge 442 m^3 s^{-1} with an unprecedented runoff response (lag time, 15'). This very flashy behaviour triggered the natural disaster as a combination of heavy rainfall (246 mm in 10 h), karstic features and land cover disturbances in the Begura de Saumà River catchment (i.e., 23 km^2). Topography-based connectivity index and geomorphic change detection were used as a rapid post-catastrophe decision-making tool, playing a key role during the rescue searching tasks. These hydrogeomorphological precision techniques were

https://doi.org/10.5194/nhess-2019-304
Preprint. Discussion started: 15 October 2019


Natural Hazards and Earth System Sciences Discussions

also applied in combination with Copernicus EMS and 'ground-based' damage assessment illustrating with high accuracy the damage driving factors in the village of Sant Llorenç des Cardassar. The main challenges in the future are to readapt hydrological modelling to global change scenarios, implement an early flash flood warning system and apply adaptive and resilient measures at catchment scale.

1 Introduction

Flash floods are related with high-intensity precipitation, mainly of convective origin and with a restricted spatio-temporal occurrence. For that reason it usually impacting at basins <1000 km^2 with response times of a few hours or less. These spatial and temporal dimensions of flash floods events are directly linked to (1) geomorphometric characteristics of the catchments and (2) activation mechanisms of runoff as a combination of intense rainfall, soil moisture and soil hydraulic properties (Versini et al., 2013). The land use modification, urbanization and recurrent wildfires can alter these activation mechanisms and the potential for flash flood casualties and damages. In Europe, 40% of the flood-related casualties in the period 1950–2006 are due to flash floods (Barredo, 2007). However, catastrophic flash-floods are much more frequent in some parts of the Mediterranean region than in the rest of Europe due to the interaction between geomorphology, climate and vegetation, contributing to create a flood-prone environment. The abrupt reliefs surrounding the Mediterranean Sea are very closeness to the coastline, shaping small and torrential catchments where the convergence of low-level atmospheric flows and the uplift of warm wet air masses drifting from the Mediterranean Sea to the coasts generate heavy downpours in very short time-spans (Gaume et al., 2009). Another cause is the reduced vegetation cover and scarce soils. Flash-floods are closely related to land use recognizing that the devastation of plant cover in the Mediterranean may increase the risk of flooding because bare soils produce larger runoff coefficients (Wainwright and Thornes, 2004).

Characterising the response of a catchment during flash flood events is important because elucidate the hydrological processes from an extreme flood and their dependency on catchment properties and flood severity (Borga et al., 2007). However, the small spatial and temporal scales of flash-floods make these events particularly difficult to monitor and document. In the case of rainfall monitoring, the spatial scales of the events are in general much smaller than the sampling potential offered by apparently dense rain networks (Borga et al., 2008; Amponsah et al., 2016). In the case of streamflow monitoring, there is a lack of flash flood discharge (Q) data from stream gauge observations (Marchi et al., 2010) although Q data are crucial to obtain representative hydrometric values and to characterize the runoff response of such extreme flash-flood events (Borga et al., 2008). In the Mediterranean region, the planning and management of flood hazards are hydro-sociologically crucial (Gaume et al., 2016), especially under the current global change context. Consequently, the hydrometric data reliability of surface water resources requires a temporal continuity and a maintenance system of the gauging stations (Fortesa et al., 2019).

https://doi.org/10.5194/nhess-2019-304
Preprint. Discussion started: 15 October 2019


Natural Hazards and Earth System Sciences Discussions

Earlier flash flood forecasting systems were based on the Flash Flood Guidance (Georgakakos, 1986), consisting in estimating the a-priori amount of rainfall needed to trigger specific Q at the outlet of a catchment, depending on antecedent wetness conditions. At the present time, semi-distributed or distributed hydrological models are more widely used for such forecasting purposes (Artinyan et al., 2016; Gourley et al., 2010; Miao et al., 2016; Nguyen et al., 2016), whilst probabilistic and ensemble modelling allow to assess the uncertainty of flash flood forecasting systems (Hardy et al., 2016). However, the uncertainty in hydrological modelling can be large and hydrological models often need to be calibrated in order to reduce the Q estimate and to understand the physical processes occurring during flash flood events (Adamovic et al., 2016; Segura-Beltrán et al., 2016; Vannier et al., 2016). Therefore, the predictability of such events remains low also adding that predictability is lowered by a high non-linearity in the hydrological response related to threshold effects (Braud et al., 2014).

It is clearly demonstrated that the understanding of flash flood processes and management further requires an integrated scientific approach (Marchi et al., 2010), encompassing (1) hydrogeomorphological precision techniques with (2) social and territorial aspects of vulnerability. Firstly, geomorphometric techniques applied to topographic surveys can be valuable planning and decision-making tools for producing flood hazard maps that are able to represent areas prone to flooding (Kalantari et al., 2017). Another application of geomorphometry and digital terrain analysis by using a topography-based connectivity index could be the simulation of preferential flowpaths for high-magnitude events to determine the main erosion and deposition areas as a tool for a better and faster response in front of catastrophic flooding events. In addition, post-storm assessments need capturing the landforms signature of the event. The use of high-resolution field measurements can be here critical to understand storm effects on fluvial dynamics (Westoby et al., 2012) and also providing input data sets for numerical modelling. This data can be difficult to obtain as traditional post-storm survey techniques are expensive or time consuming (Duo et al., 2018). In recent years, unmanned aerial vehicles (UAVs) have been used to improve traditional, expensive, or time-consuming mapping approaches on catchment science research enabling a rapid deployment and accurate high-resolution topographic data for monitoring geomorphic changes (Estrany et al., 2019).

Secondly, the concept of vulnerability relates to the predisposition of certain stakes to damage or malfunction, implying that a multitude of direct and indirect factors, often interacting in a dynamic and complex way, should be integrated in their assessment. From this point of view, vulnerability particularly relates to the damage to exposed stakes (Defossez and Leone, 2017). Particularly regarding to vulnerability, estimations of the elements at risk as well as the damage driving factors, flash floods are insufficiently understood in the Mediterranean Region, despite understanding specific and subsequent damaging processes from flash floods are developed from several European and national projects and also publications (cf. Llasat et al., 2013; Gaume et al., 2016). In addition, the largest public world databases on disaster events that contain flood events do not include all the catastrophic events occurred in the Mediterranean region (Llasat et al., 2013), emphasizing the need for further research. Since 2012, the Copernicus Emergency Management Service (Copernicus-EMS) evaluate the intensity and scope of the damage resulting in cases of natural disasters, human-made emergency situations and humanitarian crises throughout the world (Copernicus Emergency Management Service, 2019). To obtain a better understanding of the damage processes of flash floods, a comprehensive damage assessment linking hydrological process

https://doi.org/10.5194/nhess-2019-304
Preprint. Discussion started: 15 October 2019


Natural Hazards and Earth System Sciences Discussions

dynamics and intensities with damage and loss is needed (Laudan et al., 2017). As well, a comparison of 'ground-based' assessment with that Copernicus EMS one may shed light on the accuracy of this rapid and helpful tool at most of the catastrophic flash floods.

This paper aims at improving the hydrological and socioeconomic processes comprehension of devastating flash floods that frequently affects Mallorca Island (Llasat et al., 2013; Estrany and Grimalt, 2014), a paradigmatic Mediterranean flood-prone region under intense human occupation and geologically shaped by karstic features. Accordingly, the present work is focused on the catastrophic flash-flood event that hit the north-eastern part of the island, in the 9th October 2018, causing 13 casualties, the worst natural disaster in decades. The specific objectives of this study are to (1) explain the runoff response for elucidating the dependency of flood severity on catchment properties and human influences by using the flash flood *Q* data from a stream gauge installed in 2015 by the MEDhyCON Research Group; (2) assess the uncertainty of semi-distributed hydrological modelling in such severe flash flood in a karstic environment; (3) investigate the socioeconomic and territorial flood damages linked to hydrogeomorphological processes; and (4) multi-temporally analyse high resolution digital elevation models (HR-DEM) to detect and quantify geomorphic changes by using a UAV and a topography-based connectivity index for a rapid response of post-catastrophe search and rescue tasks.

2 Materials and methods

To obtain a better understanding of the flash flood as well as of damage processes, a comprehensive and combined analysis of the meteorological synoptic situation, the precipitation as well as the *Q* was developed affording the analysis of the rainfall-runoff processes at small spatial scale during this extreme event. Likewise, this analysis was linked to hydrological modelling to check the internal consistency of the information gathered by instruments and to flood damage and losses at Sant Llorenç des Cardassar village.

2.1 Study area and meteorological context of the 9th October 2018 rain event

Mallorca is a Mediterranean flood-prone region, historically affected by flash floods. Since the Late Middle Age, devastating flash floods have been systematically well documented, particularly in Palma, the capital of the island. In this town, a catastrophic event caused ca. 5000 deaths in 1403 (20% of its population), evidencing that floods are the major natural hazard in this type of environment (Petrus et al., 2018). In the rest of the island, the historical distribution patterns of human settlements had been related with fluvial systems, but always avoiding the occupation of floodplains until the increase of urban areas in the 19th century during the Industrial Revolution. However, in the second part of the 20th century this urban expansion was exponential with an increase of urban and tourist settlements (Pons Esteva, 2003) including flooding hazard areas.

In such high-energy environment, the Eastern (named 'Llevant' in Catalan language) county of Mallorca island constitutes a dramatic combination of physical and human factors to generate a flood-prone environment with a very strong coupling of

https://doi.org/10.5194/nhess-2019-304
Preprint. Discussion started: 15 October 2019


Natural Hazards and Earth System Sciences Discussions

climate and geomorphology with a constant urban expansion since 1850, with more than 10 catastrophic flash-flood events occurred during this period (Estrany and Grimalt, 2014). This county is composed by two main relief units (Álvaro et al., 1991): (1) The Llevant Ranges occupy the headwater parts with altitude ranges from 300 to 500 m a.s.l. They are constituted by a series of alpine mountains and hills that are primarily constructed of Jurassic limestones and dolomites and Cretaceous marls; and (2) The Marinas, a reefal Upper Miocene tabular platform composed of calcarenites, calcisiltites and terra-rossa postreef sediments affected by significant karstic processes endorsed to the eastern slopes of the Llevant Ranges. A morphometric analysis of the catchments carried out by Estrany and Grimalt (2014) showed differences depending on both the width of the platform (i.e., the distance between the coast and the base of the Llevant Ranges through the Miocene platform) and the hypsometry and geological settings at the headwaters. The torrentiality and clinometric variables were those more related to the geological settings. Therefore, the catchments with the highest values of torrentiality (i.e., >30) present impervious materials (i.e., lower Cretaceous and lower Miocene marls) covering approx. >40% of these catchments being located at headwater parts where the clinometry and connectivity between the slopes and channels are the highest.

The 9th October storm affected the two northernmost catchments of the Llevant County; i.e., Ca n'Amer and Canyamel Rivers (Fig. 1) with 9 and 4 casualties respectively and significant damages. The synoptic situation was like the situations generating flash-flood events in the Western Mediterranean (Fig. 2a). A cut-off low at mid-level was located in the eastern part of the Iberian Peninsula and a shallow low level pressure was affecting the same region driving warm and wet air from the Mediterranean Sea to Balearic Islands and eastern part of the Iberian Peninsula. This situation took place in early October, when the sea surface temperature is close to its annual maximum in the Western Mediterranean, providing high quantities of moisture. Moreover, the cut-off low showed a typical divergence at mid levels in its eastern flank, affecting Balearic Islands and favouring the development of deep convection. The convection initiated on the sea between the Balearic Islands and the Iberian Peninsula (Figures 2b and 2c) and due to the SW winds at mid tropospheric levels the convective cells started to move towards Balearic Islands, where they could trigger the flash-flood event after a heavy rainfall episode (Figures 2d and 2e).

This study will be focused in the Ca n'Amer River catchment (78 km^2), due to the storm struck several urban areas within it, especially the village of Sant Llorenç des Cardassar. Its main headwater tributary is the Begura de Saumà River (23.4 km^2; Fig. 1c) with altitudes ranging from 71 m.a.s.l. to 485 m.a.s.l. (Fig. 1c). The mean slope of the catchment is 16% and the length of the main channel 9.3 km (average gradient of 3%). The lithology is mainly composed by marls intercalated with limestone (60% of the area) of the Medium-Upper Jurassic as well as dolomites (22% of the area) of the Upper Triassic and Lower Jurassic (Fig. 1d). The main land use is agriculture (58%), mostly located in lowland areas. At headwaters parts, forest (26%) and scrubland (17%) are predominant, under a recurrent affection of wildfires. Due to the agricultural activity, 10% of the catchment is occupied by dry-stone terraces, most of them abandoned (Fig. 1e). The climate of the area is classified as Mediterranean temperate sub-humid, applying the Emberger scale (Guijarro, 1986). The mean annual rainfall (1968-2018, B630 AEMET station, see Fig. 1c) is 652 mm y^{-1}. Rainfall amount of 140 mm in 24 hours was estimated to have a recurrence period of 25 years (YACU, 2003).

https://doi.org/10.5194/nhess-2019-304
Preprint. Discussion started: 15 October 2019


Natural Hazards and Earth System Sciences
Discussions

2.2 Rainfall data

In order to assess the rainfall-runoff processes during the flash flood event in the Begura de Saumà River, the continuous 10-min precipitation record of the event was obtained from radar images which were initially calibrated through rainfall data downloaded at https://opendata.aemet.es/ and http://asomet.balearsmeteo.com/. Both webpages contain meteorological data for official stations of the Spanish Meteorological Agency (i.e., AEMET) and the Meteorological Association 'Balearsmeteo', respectively (see Fig. 1c: B526X-Artà-Molí d'en Leu, B496X-Son Servera, B614E-Manacor, B569X-Far de Capdepera and B603X-Colònia de Sant Pere from AEMET; and BM01-Sant Llorenç des Cardassar from Balearsmeteo). After calibration, all radar images were geo-statistically treated to obtain the hourly mean and total precipitation (and its standard deviation) fallen into regular squares of 1x1 km in size (Fig. 1c), thus allowing the analysis of the spatio-temporal distribution of the rainfall event.

The radar is located in the western part of the island of Mallorca, and it obtains reflectivity data (in dBZ) at 1*1 km of spatial resolution and at a 10-minutes temporal resolution for many altitudes. Thanks to the AEMET Open Data Platform (opendata.aemet.es), data of reflectivity corresponding to the lower Plan Position Indicator (PPI), which corresponds to an azimuth of 0.5º, can be downloaded in near-real time. Using reflectivity data, rainfall estimation was obtained by using the Marshall-Palmer relation (Marshall and Palmer, 1948).

$$Z = aR^b \quad (1)$$

where Z is the radar reflectivity ($mm^6\ m^{-3}$), R is the rain rate ($mm\ h^{-1}$) and a and b are two coefficients. As the obtained reflectivity data is in dBZ units instead of $mm^6\ m^{-3}$ a conversion was necessary using the following relation

$$dBZ = 10 * \log(Z) \quad (2)$$

The relation between Z and R depends mainly on the drop size distribution (DSD), which is usually unknown, unless disdrometer data are available, which is not the case (Chapon et al., 2008). Hence, coefficients a and b cannot be well established for this event. Multiple pair of values for a and b coefficients can be found in the literature, mostly changing between precipitation types.

We tested two pair of coefficients: (i) the pair a=200 and b=1.6 was tested because AEMET commonly uses these coefficients to obtain near-real time rainfall estimations from the same radar data that we used in this research; (ii) the pair a=300 and b=1.4 was tested because the NWS in USA used it at operational level and it is argued that these coefficients performs better in a convective environment than the first ones.

https://doi.org/10.5194/nhess-2019-304
Preprint. Discussion started: 15 October 2019


Natural Hazards and Earth System Sciences Discussions

The use of the two pair of coefficients results in the estimation of high amounts of precipitation (100 mm in the first case and 150 mm in the second case), but much lower than the maximum rainfall observation, which is higher than 250 mm, revealing the complexity of obtaining an accurate estimation of the precipitation in this event using radar data. In the scientific literature, many methodologies to enhance precipitation estimation using radar data can be found. While some methods are focused on the correction of the reflectivity data, others are based on the calibration of the estimation of precipitation using reflectivity data as these are the two main sources of errors (Harrison et al., 2000). In our study case, the combination of the distance to the location of the event (~50 km) with the 0.5º azimuth of the used PPI and the elevation of the surrounding mountains do not justify the application of techniques based on the correction of reflectivity data due to these effects. To directly correct the estimation of precipitation, geostatistical methods are commonly implemented in combination with the use of rain gauge data (Barbosa et al., 2018), but the number of available data in the most affected area is too low to implement these methods. Available data at surrounding area could be used, but due to the sharp differences in rainfall among the affected and surrounding areas we decided not to use those data.

During convective situations, high spatial and temporal gradients can be detected, both using radar data and dense rain gauge networks. As the time resolution of the radar data is 10-minutes it is difficult to assume that the obtained values of reflectivity affected the same 1*1 km area during all this time. We proposed a correction method of the rainfall estimation based on the spatial resampling, changing the spatial resolution to 2*2 km and assigning to each grid cell the value of the maximum amount of estimated rainfall at 1*1 km using the coefficients a=300 and b=1.4. As pointed out previously, using this set of coefficients leads to a relevant underestimation of the precipitation, which is compensated by the used spatial resampling method, leading to a maximum precipitation estimation > 250 mm and showing a spatial corresponding compared with rain gauge data, but with a poor spatial resolution of 2*2 km.

2.3 Discharge data

A hydrometric gauging station is located at the entrance of the Begura de Saumà River into the Sant Llorenç des Cardassar village, located 50 m upstream of the Ma-3323 road bridge (Fig. 3a). The station was built by the water authority in 1970s decade. After years of abandonment, in 2015 the MEDhyCON Research Group installed within the gauge house a Hobo Water Level U20L-04, which measures the water stage by readings of 1 minute accumulating 15-minute average values. The station is located at the very beginning of the concrete channelization of the River that crosses the village, closing a drainage basin of 23 km^2 and located ca. 50 m upstream of the first of the five bridges that cross the River within the village (see Bridge 1 in Fig. 3b). At the cross section where the hydrometric station is located, the channel bed is at 70.25 masl, whilst the top of its bank channels are at 72.00 masl.

The transformation of water stage (hereinafter WS; m) to Q (m^3 s^{-1}) through the stage/discharge rating curves (hereinafter SDRC) into the qualitative range (from low to high Q conditions) are broadly developed by power and also polynomial equations, characterised by physical-based parameters. With the absence of direct flow measurements for the Q estimation, a

https://doi.org/10.5194/nhess-2019-304
Preprint. Discussion started: 15 October 2019

Natural Hazards and Earth System Sciences Discussions

complete two-dimensional hydraulic model was applied with HEC-RAS 5.0.6 software (version November 2018), developed by the US Army Corps of Engineers, Hydrologic Engineering Center. In this case, a set of differential equations in partial derivatives that govern the flow behaviour, known as Saint Venant's equations, were solved in shallow water equations.

For the generation of the 2D hydraulic model, a HR-DTM derived from a 1 m LiDAR-based DEM dating from 2014 was used; http://pnoa.ign.es/coberturalidar. In addition, the entire concrete channelization of the Begura de Saumà River was topographically surveyed with a dGPS Leica 1200 for its integration to the HR-DTM. Within the model, all the bridges with potential flow effects on the hydrometric station were also introduced (Fig. 3a). This 2D hydraulic model was applied in a longitudinal river section established 150 m up- and downstream of the hydrometric station. Previously, the geometry of the gauging section was measured for characterizing its hydraulic functioning. It is a regular trapezoidal concrete channelization of ca. 300 m in length with low sinuosity (Fig. 3a), a longitudinal slope of 0.0052 m m^{-1}, 10 m of wide at the bed channel, being the height of embankments 1.75 m. The slope of the longitudinal section was hydraulically high, causing that the critical depth at the beginning of the channelization was the constraining factor of its hydraulic capacity (ca. 78 m^3 s^{-1}). This Q value was related with 1.75 m of WS, coinciding with the height of embankments.

As boundary conditions, an input hydrograph was arranged at the most upstream part of the studied section, whilst the WS was subsequently arranged in accordance with the slope of the channel bed at the most downstream part. Hydraulic simulations were always started with no flow conditions. Considering the hydraulic functioning characteristics for obtaining the SDRC, the calculation method used in these simulations was the Diffusion Wave. In order to design an accurate SDRC for the hydrometric station, the hydraulic effects of concrete channelization and bridges were assessed, running iteratively the model by flowing the representative Q values under stable hydraulic functioning conditions.

Accordingly, a first hydrograph was designed step-by-step by using Q values applying a power equation with 2 as exponent in a range between 2 to 512 m^3 s^{-1}. The duration of each constant Q (step) of this hydrograph was established (from preliminary simulations) in 4 hours and 15 minutes, significantly longer than the transit of the flood wave through the studied longitudinal section. In this way, the flow transit for each step in steady state conditions was guaranteed. Under these conditions and with this designed hydrograph, a first approach to the SDRC was obtained. In order to improve the accuracy of the SDRC, a second hydrograph was designed, also containing the Q values of the first hydrograph. For optimizing time consumption of the modelling, this second hydrograph was performed with constant Q (step) of shorter temporal duration; i.e., 1 and 2 hours depending on the Q range.

The SDRC was divided into two sections. The first one was related with a scenario where bridges do not impact on the hydraulic functioning at the gauging section, despite flow being bankfull or even overbanking the channelization. The second one was a scenario under the influence of bridges; i.e., flow functioning below them and also over their decks. It is then clear that the design, dimensions and proximity to the hydrometric station of these bridges caused a direct influence on the flow behaviour in the hydrometric station due to they were affected by obstruction (see pictures in Fig. 3). The obstruction of the Bridge 1 was produced when the upstream section of the concrete channelization reached the bankfull, so the dragging and floating elements began to collide against the beck of the bridge, triggering the obstruction process.

https://doi.org/10.5194/nhess-2019-304
Preprint. Discussion started: 15 October 2019


Natural Hazards and Earth System Sciences Discussions

Consequently, it was necessary to integrate in the hydraulic model those obstructions observed in the downstream bridges, at least in the two nearest ones (Fig. 3a). In detail, 85% of obstruction in the Bridge 1, 40% in the Bridge 2 and without obstruction for the other ones. The overbank flow coefficients were 2.2 for bridges 1, 4 and 5, and 2.1 for bridges 2 and 3. The obtained SDRC allowed to calculate this phenomenon which is activated with Q values ranging 130-160 $m^3 s^{-1}$. Nevertheless, a calibration in the hydraulic model of overbank flow coefficients and the degree of obstruction of these structures was needed by using complete flow equations (Full Momentum) and without changes in boundary conditions. For this purpose, the WS calculated in open channel conditions were compared with those WS observed in the field during and after the event in the hydrometric station and its surrounding floodplain area. Accordingly, ground control points in three representative locations around the hydrometric station were selected (Fig. 3b), also considering the maximum WS reached in the hydrometric station (4.55 m). The modelling results in open-channel conditions for the ground control points involved an error <5% error in WS or even <1% in the case of the WS recorded at the hydrometric station.

The SDRC was finally designed (see Fig. 4), clearly illustrating the two differentiated sections with a gap between them in WS of ca. 1.5 m because 1.4 m is the edge of the Road Bridge 1 just located 50 m downstream of the hydrometric station. The SDRC is fitted to a power equation for both sections, obtaining high values of significance ($R^2 > 0.990$). Thus, in the case of the first section of the SDRC, the adjustment was R^2 0.999, operating in open channel flows up to 160 $m^3 s^{-1}$ in bankfull or even overbanking the channelization but always without the bridges influence. The second section, with a R^2 0.996, defined for $Q > 160$ $m^3 s^{-1}$, was already influenced by the presence of the bridges. That is in open channel flows but conditioned by the backwater generated in the flowing under pressure inside the span of the Bridge 1 as well as over its concrete decks.

2.4 Hydrological modelling

A semi distributed hydrological model was used to reproduce the hydrological response of the catchment during the flash-flood event; i.e., the Routing System (RS) model (García-Hernández et al., 2007; Jordan, 2007). Therein, the GSM-SOCONT was the used rainfall-runoff model, comprising an appraisal of hydrological processes such as snowmelt as well as surface and subsurface infiltration-induced flow and groundwater flow due to percolation (Jordan, 2007; Schaefli et al., 2005). The catchments were divided into elevation bands to incorporate the influence of temperature evolution with altitude and orographic effects within mountainous catchments. In this model, the sub-catchments were divided into 100 meter elevation bands. The GSM-SOCONT model was applied to each elevation band, which were summed at the outlet of each sub-catchment. The input data of the GSM-SOCONT was the temperature obtained from meteorological stations and the precipitation derived from radar measurements (see previous section).

The scheme of the GSM-SOCONT model is shown in the Fig. S1. First, the precipitation and temperature were interpolated for each elevation band based on inverse distance weighing using the Shepard method (Shepard, 1968). In this study, all the interpolated precipitation was directly transferred to the soil infiltration model. The soil-infiltration model was based on

https://doi.org/10.5194/nhess-2019-304
Preprint. Discussion started: 15 October 2019


Natural Hazards and Earth System Sciences Discussions

modified GR3 equations (Schaefli et al., 2005). Infiltration and evaporation were determined by the soil saturation; i.e., infiltration is higher for lower soil saturation whereas evapotranspiration is higher for high soil saturation. Surface runoff was computed with the SWMM model. The soil-infiltration was modified to simulate karstic hydrological dynamics, as shown in the Fig. S2. The precipitation was infiltrated in the soil as in Schaefli et al. (2005) as a function of soil saturation (Fig. S2a). The resulting outflow from the reservoir (Q_{GR}) is also depending on the soil saturation, with increasing outflow with higher soil saturation. In the modified equations, the soil saturation can increase up to a certain level ($H_{GR,threshold}$), being a parameter to be adjusted in the model (Fig. S2b). When this threshold is reached, the soil reservoir releases all the available volume contained between the $H_{GR,threshold}$ and the minimum water level (k_{karst} in Fig. S2c). The released volume of water is then transferred to the SWMM model, described in (Schaefli et al., 2005). The relevant parameters for the modified version of the soil infiltration model were the maximum soil capacity ($H_{GR,max}$), the threshold for the karstic behaviour ($H_{GR,threshold}$) and the release coefficient (k_{karst}).

2.5 Damage assessment

Rapid Mapping is a mature Earth Observation (EO) service with many years of user oriented development since the International Charter `Space and Major Disaster' was established in 1999. This activity of providing EO satellite data derived disaster mapping during emergencies to civil protection and humanitarian user communities occurs at national, continental and worldwide scales. Considering the extreme helpfulness of the Copernicus EMS reports performed by using rapid mapping techniques, the damage assessment of the event was focused on the comparison between two information sources. The first one, a 'ground-based' report, was the damage analysis carried out by the Directorate General of Emergencies of the Balearic Islands Government (Pol, 2019). This 'ground-based' report provided a detailed description of the resources mobilized in the emergency phase and also a damage inventory. The second information source was the 'remote-based' damage assessment carried out by Copernicus EMS (https://emergency.copernicus.eu/mapping/ems-product-component/EMSR323_01SANTLLORENC_02GRADING_MAP/2), also including the flooded areas established by Copernicus EMS within the Sant Llorenç des Cardassar village.

The damage assessment comparison between the two sources was developed applying a cartographic overlay with GIS tools. In order to provide more accuracy, detailed territorial information and also flow direction were also incorporated. Firstly, the type of buildings and land uses at urban plot scale from the General Directorate for the Cadastre (http://www.sedecatastro.gob.es/). Secondly, an estimation of the flow direction with Arc Hydro Tools (ESRI, 2019) in the urban network were used to assess the role of hydrological processes in damaging. The results are presented through a set of tables and cartographies that summarize the effects of the event and help to reflect on its causes and consequences.

https://doi.org/10.5194/nhess-2019-304
Preprint. Discussion started: 15 October 2019


Natural Hazards and Earth System Sciences Discussions

325 **2.6 Sediment Connectivity and geomorphic change detection**

Besides the hydrogeomorphological monitoring tasks, the 15th October 2018 MEDhyCON Research Group was incorporated to the Emergency operational to collaborate in the search of a missing person during the flash flood who had not been found yet by then. Firstly, and taking into consideration the emergency situation, the index of (water and sediment) connectivity at the catchment scale was applied to find out the areas with the greatest sediment deposition potential. The sediment
330 connectivity index (IC) proposed by Borselli et al. (2008) and modified by Cavalli et al. (2013) was applied to determine the preferential flux-paths by exploring the water and sediment transference patterns between different landscape compartments of the entire study catchment; Ca n'Amer River. In this way, the IC is a dynamic property of the catchment that indicates the probability of a particle at a certain location to reach a defined target area, which in this study was established at the catchment outlet (Trevisani and Cavalli, 2016). This morphometric index was mainly derived from a HR-DTM, in this case,
335 a 1 m LiDAR-based DEM dating from 2014; http://pnoa.ign.es/coberturalidar. IC was calculated as follows:

$$IC = \log10\left(\frac{D_{up}}{D_{dn}}\right) = \log10\left(\frac{\overline{W}\,\bar{S}\,\sqrt{A}}{\sum_i \frac{di}{Wi Si}}\right) \quad (3)$$

where D_{up} and D_{dn} are an up- and downslope components respectively, $\bar{S}$ average percentage slope, A the size of the upslope contributing area, $\overline{W}$ an averaged weighting factor representing terrain roughness and a flow length di of the ith cell along the steepest downslope direction. IC was calculated by using the freely available *SedInConnect* (Version 2.3) software
340 developed by Crema and Cavalli (2018).

Secondly, in addition to the ability of HR-DEMs in facilitating the improvement of the sediment connectivity as a powerful tool to determine the preferential flux-paths, the present study evaluated the landforms signature of the event by using UAVs as a tool for a rapid response of post-catastrophe search and rescue tasks. The latest technological advances in remote data acquisition (i.e., UAVs) and topographic modelling (i.e., Structure for Motion –SfM– and Multi-View Stereo –MVS–) led to
345 a huge advance in Earth and environmental sciences. Following the incorporation of MEDhyCON to the emergency operative, several UAV flights were carried out all along the Ca n'Amer River, from the headwaters (Begura de Saumà River) to its outlet into the Mediterranean Sea at the village of S'Illot (Fig. 1c). This fieldwork involved the establishment and survey of more than 250 ground control points (GCPs), needed for an appropriate geo-referencing of the aerial photographs taken by the drone. Therefore, on 15th October 2018, just six days after the flash flood, evidence of erosion was
350 recorded by aerial photographs taken with a small unmanned aerial vehicle (UAV *DJI Phantom 4 Pro*, < 2 kg) and its conventional camera. The sensor dimensions are 12.83 x 8.60 mm, 5472 x 3648 px. The camera was calibrated by means of the *Agisoft Lens*, an automatic lens calibration routine included in *Agisoft Metashape* that uses LCD screen as a calibration target and enables the full camera calibration matrix, including non-linear distortion coefficients (*Manual* Agisoft Lens, 2018), to be calculated. Resolution was set at 20 Mpix, shutter speed at 1/2,000 s and focal length was 8.60 mm. Most of the
355 active zones of the main stream –including the floodplain corridor– with evidence of erosion and deposition were surveyed also ensuring the recording of high-water marks.

https://doi.org/10.5194/nhess-2019-304
Preprint. Discussion started: 15 October 2019


Natural Hazards and Earth System Sciences Discussions

Imagery acquired during the aerial campaign enabled (1) the creation of mosaics of aerial georeferenced images and (2) the generation of high-resolution digital terrain models (HR-DTM) with a cell size of 0.05 m. These were produced by *Agisoft Metashape Pro® v1.5.3* using automated digital photogrammetry techniques. This software obtains high-quality results easily from algorithms known as 'Structure-from-Motion' (SfM). Further details on the implemented algorithms can be found in Lowe (2004) and Westoby et al. (2012). For the proper acquisition of the imagery, flight altitude was set at 70 meters, ensuring ground resolution close to 0.02 m pix^{-1}, and the camera was programmed to shoot every 15 m, flying at an average speed of 5 m s^{-1}.

Once all the drone images were geo-referenced and properly mosaicked, topographic modelling (i.e., Structure from Motion) was applied to generate the post flash-flood very-high resolution DEM (i.e. 5 cm pixel size). The comparison of that DEM to that of the catchment prior to the catastrophic event (LiDAR-based DEM dating from 2014) allowed the quantification and assessing of the actual magnitude (competence) of the event in terms of, e.g., volume of sediments eroded and/or deposited, alteration of the fluvial morphology. Consequently, geomorphic changes were estimated in a downstream floodplain of the Sant Llorenç des Cardassar to evaluate the amount of overbank sedimentation in the area of the rescue where IC suggested the search. The measurements were developed using a procedure, similar to DoD, comparing the elevation of the ground class points extracted from the LiDAR topography collected in 2014 (http://pnoa.ign.es/coberturalidar) and the points extracted from the 0.05 m resolution DEM obtained by UAV flight in the same coordinates. Errors (RMSE) in xyz of the UAV DEM was calculated for 12 precise coordinates' points (different from those GCPs used for image geo-reference) within the floodplain area of volumetric measurements being < 0.175 m.

3 Results

3.1 Catchment hydrological dynamics

The hydrogeological and geomorphological characteristics of the Mallorca river catchments control its surface water/groundwater interaction hence generating different streamflow regimes (cf. Estrany et al., 2009). The headwaters of all sub-catchments and the tributaries that drain the Llevant Ranges and Marinas are ephemeral due to the high degree of fracturing, fissuring and karstification, favouring infiltration and percolation through perched karstic aquifers unconnected from the main stream channels.

The hydrological monitoring period in the hydrometric station was from 10th January 2015 to 30th September 2018 (Fig. 5), excluding the October 2018 month when the catastrophic flash flood event occurred (see results in sub-section 3.2). This gives a series of almost 4 hydrological years under hydrometeorological conditions illustrating an ephemeral behaviour of the Begura de Saumà River, being on average in terms of precipitation (see the inset table of Fig. 5). In terms of *Q*, this inset table also shows the behaviour during study period of different hydrological parameters. However, these values are not possible to be compared at long-term due to errors of up to two orders of magnitude in *Q* values measured by the hydrometric network managed by the Balearic Islands Government (cf. Fortesa et al., 2019). Events of different magnitudes

https://doi.org/10.5194/nhess-2019-304
Preprint. Discussion started: 15 October 2019


Natural Hazards and Earth System Sciences Discussions

occurred during this study period, some of them representative of recurrence ≈ 5 years in terms of rainfall. However, only two events recorded peak Q (hereinafter Q_{peak}) values > 1 $m^3 s^{-1}$, both occurred in January, when the hydrological pathways were completely active due to saturation processes. In January 2015, with 120 mm of rainfall within 48 h at the AEMET-B630 Ses Pastores rainfall station (see location in Fig. 1), generated a flow response with a Q_{peak} of 2.8 $m^3 s^{-1}$. Finally, 153 mm of rain were accumulated in January 2017 within 72 h with a Q_{peak} of 4.8 $m^3 s^{-1}$, the maximum recorded in the hydrometric station during the study period before the catastrophic flash flood.

3.2 Hydrological response of the flash flood

The duration of the rainfall event was ca. 10 h and the average catchment rainfall amount was 246 mm for both the Blanquera and the Begura de Saumà catchments. Average and maximum rainfall intensities in 10 minutes were respectively 24 mm h^{-1} and 46.4 mm h^{-1} (Table 1a). However, spatial differences in rainfall depth within the catchments can be observed. In this way, the total rainfall amount ranged spatially within the catchment from 170 mm (see R1 Fig. 6) to 285 mm (See R5 and R6 Fig. 6), being the highest rainfall amount in 1 h at R12 (i.e., 77.2 mm). These highest rainfall values occurred at the headwater parts of the Begura de Saumà River catchment (i.e., R12 Fig. 6) during the beginning of the event; i.e., 15:00 h. At 17:00 h, the convective train was moving very slow causing that a new peak of rainfall amounts in 1 h were located in the downstream part of this catchment with values between 60 and 70 mm recorded at R5, R6 and R9 (Fig. 6). During the last part of the event, at 19:00 h, rainfall amounts in 1 h of 60 mm h^{-1} were recorded from R2 to R5.

Rain started to fall at 15:00 h (official time; UTC + 2 h). At 18:00 h, its amount was already 104.2 ± 20 mm h^{-1}, but the runoff response was insignificant with Q i.e. 0.089 $m^3 s^{-1}$. However, one hour after, at 19:00 h, with rainfall reaching an amount of 144.6 ± 36.8 mm h^{-1} Q was already bankfull; i.e., 120 $m^3 s^{-1}$ because soil infiltration capacity of the catchment was likely exceeded promoting a rapid overland flow generation. Consequently, only 15 minutes later, Q_{peak} was recorded (i.e., 442 $m^3 s^{-1}$) and hence triggering a catastrophic flood. Furthermore, Q values continued being high (i.e., > 135 $m^3 s^{-1}$) until 20:45 h due to the convective train maintained rainfall intensities > 24 mm h^{-1}. At 00:00 h, the rainfall event finished and Q being sharply reduced to 0.016 $m^3 s^{-1}$. The table 1b summarizes the most important runoff parameters, shedding further light on the hydrology of this flash-flood event.

3.3 Hydrological modelling

The hydrological model previously described was used to better understand the process during the event. The results of the hydrological model simulation can be seen in Figure 6. The input data used in the model was the continuous radar dataset described previously and the temperature measured at the surrounding meteorological stations; i.e., three stations located within a radius of 12 km. The model was calibrated to reproduce the event and the final parameters were set to:

- $H_{GR,max}$ = 1.4 m

https://doi.org/10.5194/nhess-2019-304
Preprint. Discussion started: 15 October 2019

- $H_{GR,threshold}$ = 0.215 m
- K_{karst} = 0.045 m
- Initial conditions of the GR reservoir: $H(t_0)$ 0.08 m, corresponding to a low soil saturation.

The relative volume error was 6% between the simulation and the measurement. The simulated peak ratio was of 437.7 $m^3 s^{-1}$; with an estimated runoff coefficient of 37.8%. The recession limb was not as sharp as the measured *Q*. It is worthy to be noted that it was not possible simulating *Q* under the same magnitude as the measured *Q* during the episode with a non-modified version of the GR3 model.

The same parameters were applied over the entire headwater catchment. Accordingly, the Q_{peak} from the other headwater tributary located on the west flank of Sant Llorenç des Cardassar village (Sa Blanquera) was estimated by the model to be 77.2 $m^3 s^{-1}$, corresponding to an estimated runoff coefficient of 22.7%.

3.4 Damage assessment

The flash-flood caused a high social and economic repercussion in the Llevant County and the whole Mallorca Island, as well as an extensive national and international media coverage. The flash-flood event was a catastrophe with 13 deaths and economic damage of great importance on the population and infrastructure. This number of casualties impacted the national and international opinion in one of the most important international touristic resorts, considered traditionally safe. For further assessment on the media impact, see Table S1.

The damage assessment report carried out by the Emergency Services of the Balearic Islands Government illustrated an unprecedented mobilization of resources in the Region during the first week after the catastrophe in according to the high number of victims and damages (Table 2; Pol, 2019). The declaration of disaster area is regulated by the Spanish Law 2/2018 and Decree 33/2018 (BOE, 2018). This law establishes public support for alleviating the basic needs of families, deaths, housing assistance, and aids for loss of vehicles and also support for the affected economic sectors. The law additionally aid for the reparation of public infrastructure and environmental damage, also specifying the amount of aid and its administrative procedure. The initial costs of the emergency works exceeded 25.5 million € including the following actions: cleaning and restoring river channels, demolition of walls and structures affected, removal of potential polluting sources (GOIB, 2018). In parallel, the Insurance Compensation Consortium (CCS, 2018) is the Spanish public agency for managing payments to affected people in cases of damage caused by catastrophic events. This agency published in December 2018 a list of processed dossiers in this flash-flood as well as the total amount of payments considering the damage assessment after the disaster in the Sant Llorenç des Cardassar village. A total of 1,830 dossiers were processed, being paid an amount of 5,392,540 € (see Table S2).

A territorial and hydrological analysis of the damage assessment is here developed. The location of the affected buildings and the WS reached in the streets and buildings provided by the DG of Emergencies of the Balearic Islands Government and by Copernicus EMS allowed to map three different affected zones within the urban area of Sant Llorenç des Cardassar

https://doi.org/10.5194/nhess-2019-304
Preprint. Discussion started: 15 October 2019


Natural Hazards and Earth System Sciences Discussions

(Figure 7a). Zone 1 is produced as a result of the overbank flow of the Begura de Saumà River and corresponds mostly to the delimitation of affected areas carried out by Copernicus EMS. In this Zone 1, the highest WS in the streets was reached, exceeding 3.3 m. The Zones 2 and 3 corresponding to those urban areas affected by the overbank flow of the Sa Muntanyeta Creek, located in the northernmost area of the village. The streets of Sant Llorenç des Cardassar rerouted the overbank flow from both the Begura de Saumà River and the Sa Muntanyeta Creek (Fig. 7b and 7c), causing significant damages to vehicles and public movable goods. In addition, most of the buildings of Sant Llorenç des Cardassar use the ground floor as a home or business, so the event caused a major inundation of water and mud disabling its use and requiring tasks of cleaning and restoring. In according to the Balearic Islands Government, 392 damaged buildings and plots were inventoried at the urban area of Sant Llorenç des Cardassar, being located most of them in the Zone 1 (Figures 7d and 7e). The flow direction illustrated how the N-> S direction, parallel to the Begura de Saumà River, was that caused the most damage in the Zone 1, with 348 affected buildings and a WS average of ca. 1.03 m. The Zones 2 and 3 showed lower intensity damage, being 37 and 6 the affected buildings and a maximum WS of 1.80 m and 1.60 m respectively. In these Zones 2 and 3, the flow direction did not illustrate a clear pattern because Sa Muntanyeta Creek is a small catchment (i.e., 2.2 km^2) and the urban street network and parcels are not parallel to its natural flow direction.

The cartographies included in the Balearic Flood Risk Management Plan (GOIB, 2016) indicate the urban area of Sant Llorenç des Cardassar as a maximum risk area. Accordingly, the Plan developed an analysis of the potentially affected areas by recurrence periods of 10, 100 and 500 years (Figure 7f). In addition, Table 3 summarizes the damaged buildings analysing if they are included in this official flood risk areas in according of the explained recurrence periods. None of the flood risk maps for different return periods encompassed the areas affected as a result of the event. The 10-year recurrence map only includes 25% of the affected areas; the 100-year covers 48% of these damages while the 500-year map only reached the 60% (Table 3).

Comparing the affected zones where damaged buildings are also depicted with the Copernicus EMS delimitation, some differences between the initial flash-flood delimitation carried out by Copernicus EMS-EU and the distribution of damaged buildings can be observed (Figure 7f) in Zones 2 and 3. It is worthy to be noted that the post-event delimitation of Copernicus EMS (Copernicus Emergency Management Service, 2018) covered ca. 90% of the real damages.

3.5 Sediment Connectivity and geomorphic change detection as emergency tools

The search of the only missing person during the flash flood who had not been found yet 6 days after the storm produced a high social impact in the Balearic Islands and beyond. Subsequently, the application of hydrogeomorphological precision techniques was crucial with a very intense topographical survey carried out to build very-high resolution (i.e. 5 cm pixel size) digital elevation models and ortophotomosaics.

Firstly, and taking into consideration the emergency situation, the index of (water and sediment) connectivity at the basin scale was applied to find out the areas with the greatest sediment deposition potential (Fig. 8a). The IC allows a better

https://doi.org/10.5194/nhess-2019-304
Preprint. Discussion started: 15 October 2019

understanding of the sediment transfer processes within drainage catchments. The most connected areas of a basin are those in which their different compartments are more powerfully linked. That favours a largest water surface fluxes generation, thus erosion and, potentially, larger soil losses. Contrarily, the zones with low connectivity are those in which their topographical characteristics disconnect the water and sediment fluxes, acting like storage or deposition areas. The IC was applied to the whole Ca n'Amer River basin but it was just analysed from the point where the missing person was last seen (Fig. 8b, point 1). That was the exact point where the car in which he was circulating was swept away by the flood-wave. Therefore, the preferential water and sediment paths which were most likely followed by the flood fluxes were identified, as well as the most important deposition areas downstream from the person's last-sight point. Such most likely deposition zone was identified, and immediately communicated to the Emergency Authorities, upstream from the bridge of the road Ma-15 which crosses over the Ca n'Amer River around 1 km below the Sant Llorenç des Cardassar village. Then the searching activities were concentrated at that precise area where the last victim was actually found (Fig. 8b, point 2) when Emergency Authorities had decided to move these searching activities to the debouching area of the Ca n'Amer River and beyond into the Mediterranean Sea.

In addition to the ability of HR-DEMs in facilitating the improvement of the sediment connectivity as a powerful tool to determine the preferential flux-paths and deposition areas, the present study evaluated the landforms signature of the event by using UAVs as a tool for a rapid response of post-catastrophe search and rescue tasks along the whole downstream section of the Ca n'Amer River from the village of Sant Llorenç des Cardassar in order to effectively quantify the sediment deposits generated by the flash-flood and locating and quantifying the most important deposition areas downstream from the person's last-sight point. As the last missing person was found with the application of connectivity index, the sediment deposition quantification was finally not necessary during the Emergency operational. However, in this study, the assessment was carried out at the floodplain area where this person was found in order to check its validity. Accordingly, for each of the 7103 LiDAR points included in the right back of the Ca n'Amer River the elevation was compared, and from the differences interpolated (TIN) an elevations raster from which a total volume of 844.28 m^3 was calculated, for an area of 12,254 m^2. The irregular distribution of the sediments in Fig. 8d responds to the rescue mobilisation. In the gaps visible in the sedimentation area of the Fig. 8d vehicles and search machinery where removed and not included in the volumes.

4 Discussion

4.1 Hydrological response and flash flood modelling in small Mediterranean karstic catchments

The flash flood event described in this study fits with the monthly distribution of flash floods in Spain carried out by Gaume et al. (2009), being October the month with the highest number of this flood type events. Furthermore, the hydrological characteristics of the event were comparable with the flash flood requirements established by Amponsah et al. (2018) to be included to the EuroMedeFF database, which are a unit Q_{peak} higher than 0.5 $m^3\ s^{-1}\ km^2$, a spatial extent lower than 3,000

https://doi.org/10.5194/nhess-2019-304
Preprint. Discussion started: 15 October 2019


Natural Hazards and Earth System Sciences Discussions

km^2 and a storm duration shorter than 48 h. In this case, the unit Q_{peak} was 19 m^3 s^{-1} km^2 and the storm duration 10 h. In addition, the characterization of 60 extreme flash flood events carried out by Marchi et al. (2010) offers a frame to compare the event of Begura de Saumà River with other flash floods regarding the rainfall amount, rainstorm duration, catchment area, lag time, runoff coefficient and unit Q_{peak}. With a rainstorm duration of 10 h and a mean rainfall amount of 246 mm, the event is located within the flash flood group events with highest rainfall intensities, which is a key factor for extreme events due to controlling the magnitude of the runoff response. This group of events is mainly composed by Mediterranean and Alpine-Mediterranean catchments. The relationship between catchment area and lag time or response time exceeded any flash flood reported until nowadays. The lag time of the event (0.25 h) was significantly lower than the lower limit defined through envelope curves. This short response time was caused by a combination of geographic characteristics of the catchment as well as the occurrence in time and space of maximum rainfall amounts and intensities (Fig. 6), as it has been depicted in sub-section 3.2. In addition to rainfall characteristics, other factors that play a key role over flash floods are lithology and antecedent wetness conditions. On the one hand, low runoff coefficients have been reported in karst areas with carbonate lithology due to high infiltration rates (Li et al., 2019). On the other hand, Marchi et al. (2010) reported differences in the median runoff coefficient up to 23%, which were higher on flash floods occurred under wet antecedent conditions. The flash-flood event of the Begura de Saumà River occurred under dry antecedent conditions because the rainfall amount 9 days before was only 6.4 mm in a period when evapotranspiration was still high as temperatures were quite warm (i.e., 20ºC). Despite these antecedent wetness conditions, the runoff coefficient of the event (i.e., 36%) was analogous to the median runoff coefficient under average conditions (37%) than dry ones (20%), as reported by these authors. This response illustrated the key role of rainfall intensity in the generation of a high Q_{peak} (i.e., 442 m^3 s^{-1}) with a high potential to generate geomorphological changes. In this way, the unit Q_{peak} obtained (i.e., 19 m^3 s^{-1} km^2) can be classified as the third highest value of all the reported values in Marchi et al. (2010) and the highest of those values obtained from streamflow measurements in a hydrometric station and not by post-event analysis.

The hydrological model has been calibrated specifically for the flooding event. The parameters of the modified GR reservoir as well as the initial conditions were adjusted to best represent the flooding event. A very sensitive parameter is the $H_{GR,threshold}$, which regulated the time when additional water reserve in the soil was released. Modelling results were also very sensitive to initial conditions (soil saturation) before the rainfall event. During the calibration process, it was necessary to simulate, on one hand, smaller flood events observed at the hydrometric station. On the other hand, the model had to reproduce the historical 2018 flood event. However, the flood event could not be reproduced when the model was calculated for a long time period, due to initial conditions that were not adjusted prior to the event. In this context, the initial condition $H(t_0)$ was adjusted manually. The uncertainty for the results regarding Sa Blanquera River was higher because the lack of hydrometric data in this catchment. There was no karstic behaviour of the model within this subcatchment, which was the main modelling uncertainty for this ungauged subcatchment. The model analysis clearly showed that without any massive water storage during the first part of the rainfall event, which was released at the Q_{peak} of the event, it was impossible to reproduce the correct flood magnitude and the very short lag time. This water storage can be due to underground karstic

https://doi.org/10.5194/nhess-2019-304
Preprint. Discussion started: 15 October 2019


Natural Hazards and Earth System Sciences Discussions

volumes combined with pipes, or storage / dam break effects. Only future large flood events will allow us to validate the chosen parameters, as the 2018 flood event was the only one needing a karstic component in the rainfall model to be correctly represented by the model.

The predictability of flash-flood events is a non-solved issue, especially because forecasting of intense thunderstorms is also non-solved for operational meteorology. Even using one of the best state-of-the-art weather forecasting models, Harmonie/AROME, the Spanish National Weather Service (AEMET) only activated a yellow warning for one-hour accumulated precipitation of 20 mm beforehand. On the other hand, the synoptic situation was well forecasted by global forecasting models some days before the event. An experimented forecaster could anticipate the occurrence of intense thunderstorm using these models, but without any quantitative or geographical precision, which are two key factors in flash-flood forecasting. However, nowcasting products, based on radar, satellite and ground-truth may allow a better anticipation of severe weather situation. These products are updated at a high frequency (several minutes to one hour) and compensate the weather forecasting models which are updated with a lower frequency. The main challenge to apply the hydrological model in an early flash flood warning system is a good estimate of initial conditions of the soil saturation as well as accurate rainfall forecasts. For the latter one, the scientific community is working on now-casting products that typically deliver short-term (few hours lead time) rainfall forecast which are updated on a high frequency, from 10 minutes to an hourly base. These forecasts are based on real time measurements which combine data from radars, satellites and meteorological stations. On the other hand, it is hard to automatically estimate initial conditions as the river is dry most of the time and without soil moisture measurements in the catchment. Data assimilation and automatic adjustment of initial conditions, which are usually applied in operational forecasts, are therefore not relevant here. However, an early warning system can be built using the model proposed in this paper by assessing the uncertainty of the forecast, for instance by using different scenarios of initial conditions of soil saturation. Since the proportion of rainfall lost as runoff rises significantly as the percentage of vegetation cover falls below about 30%, bare soils produced a large runoff coefficient. Moreover, soils in the Mediterranean often have low infiltration capacities because the soils dry out in the summer, following the winter moisture. Fine surface “seals”, ca. 1-2 mm thick, may increase the runoff rates. Sometimes evaporation leads to chemical as well as mechanical seals (often of calcium carbonate) that again reduce infiltration rates vary dramatically. Mediterranean soils with high erosion rates also often have stones exposed at the surface (Schoorl et al., 2004). The stony soils create higher runoff rates and lower infiltration rates when rock fragments are poking out on the surface (Poesen and Lavee, 1994). A hydrology knowledge suggests that flooding is intimately related to land use and that the progressive history of the devastation of plant cover in the Mediterranean is likely to enhance the flood risk (Wainwright and Thornes, 2004). These factors are a major reason for concern about desertification. Moreover, thicker soils can hold more water if they are permeable and as the soil is eroded, this storage is reduced to produce a downward spiral of more runoff, more erosion and more flooding. The removal of vegetation by fires has a similar effect (less interception, less soil storage) and this has been experimentally documented after major fires. In the first few years runoff is usually observably higher because the soils are made hydrophobic (water-resisting) by fire and because there is less vegetation and less soil to store the rainfall.

https://doi.org/10.5194/nhess-2019-304
Preprint. Discussion started: 15 October 2019

4.2 Flood damages and hydrogeomorphological techniques as decision-making tools for a rapid response of post-catastrophe operations

The incorporation of MEDhyCON research group the 15th October 2018 to the Emergency operational allowed the application and testing of hydrogeomorphological precision techniques. The fundamentals are that flood risk plans and Emergency activities are based on a thorough understanding of linkages between sediment and catchment compartments at all stages of flood events. Integrating topography-based connectivity assessment (Kalantari et al., 2017) and geomorphic change detection can be crucial to support decision making in flood risk planning and also in Emergency survey as it has been demonstrated in this study. The combination of hydrological and sediment connectivity (IC in various forms) with other key natural characteristics (i.e., soil type and topography by using LiDAR-based HR-DEM) as well as the integration of territorial information such as land cover/uses by using Cadastre data bases (Piaggesi et al., 2011) has resulted a powerful tool as it has been demonstrated in this study. Besides, the post-event delimitation and damage assessment released by Copernicus EMS (Copernicus, 2018) allowed the identification of ca. 90% of the real damages in this traditional Mediterranean village such as Sant Llorenç des Cardassar composed by compact blocks of buildings and plots. The Synthetic Aperture Radar (SAR) technology with very high spatial resolution (1-3 m; Plank, 2014) is fundamental to obtain a high efficiency and accuracy of this rapid mapping tool at low cost. Consequently, Emergency resources can be directly concentrated on the most damaged areas without the need of checking the entire affected area on the ground.

The increase in the torrentiality of rainfall as a result of climate change in the Mediterranean region may exacerbate the level of exposure to floods of urban areas and infrastructures causing an increase in quantity and also in intensity of catastrophic events. Public administrations should develop a continuous adaptation of prevention and management flood risk tools to these new scenarios. The legal framework for flood risk planning and management evidenced that the level of risk exposure was extensively known. In addition, the analysis of current regulations shows that the appropriate preventive measures were being taken to minimize possible damage in a potential event in the Balearic Islands. However, the magnitude of this flash-flood exceeded any type of forecast carried out by the risk and emergency plans. The consequences of this catastrophe evidenced deficiencies in prevention tasks by the Public Administration, both at the level of urban planning and infrastructure as well as in the risk management itself. In addition, population was also not prepared due to a very low level of risk culture.

5 Conclusions

The hydrogeomorphological analysis and damage assessment developed in this paper has provided a comprehensive understanding of the Sant Llorenç des Cardassar flash flood event occurred in the 9th October 2018 by means of an integrated approach with a meteorological, hydrological, geomorphological, damage and risk data analysis. The use of rainfall radar

https://doi.org/10.5194/nhess-2019-304
Preprint. Discussion started: 15 October 2019

data –corrected with rainfall stations measurements from the surrounding region– combined with *Q* data from stream gauge observations elucidated how spatio-temporal distribution of rainfall amounts and intensities, karstic features and land use/cover resulted in an unprecedented very flashy runoff response in a Mediterranean environment, triggering this natural disaster. It was shown that the application of different direct estimation approaches may reduce the uncertainty of hydrological modelling and thus increase the credibility and practical value of the whole analysis. Without a doubt, the inclusion of streamflow monitoring data proved to be crucial in this flash-flood type event thorough an accurate calibration with two-dimensional hydraulic model also integrating the influence of bridges obstruction in flow routing.

The flash-flood event was a catastrophe that caused 13 casualties, huge economic damages and an unprecedented human resources mobilization in the Balearic Islands Region. Rapid mapping from Copernicus EMS and detailed damages reported by regional authorities linked to territorial information from Cadastre and hydrogeomorphological processes illustrated with high accuracy the damage driving factors in the urban area of Sant Llorenç des Cardassar village. Despite the flood risk planning evidenced the high level of risk exposure, the disaster was generated by a very high exposure of buildings and infrastructures to floods, the absence of early warning systems with efficient action protocols in case of flood emergency, and the lack of municipal regulations to instruct the population on how to act when occurring an event of this magnitude. The incorporation of hydrogeomorphological precision tools during Emergency post-catastrophe operational has been revealed as a powerful tool. Then, the simple application of a geomorphometric index from easy-access LiDAR-based topographic data resulted in a rapid identification of deposition zones in the different compartments of a catchment helping in the search and rescue of missing persons. In addition, the evaluation of landforms signature by using UAVs effectively quantified the sediment deposits generated by the flash-flood and/or mobilised by the Emergency operational during the rescue searching tasks.

This study represents a first step to further improve flash-flood management in Mediterranean flood-prone regions such as Mallorca in the future under the global change effects, as they have major consequences in terms of risk management. Mediterranean regions are subject to violent flash floods that could be intensified –especially in terms of peak discharge– in the future due to forest fire, land uses and/or climate changes. These future consequences of global change should be considered in future flood warning systems and flood policy with the modification and adaptation of hydrological and flood risk models allowing the development of a rule-based system with adaptive and resilient measures at catchment scale.

https://doi.org/10.5194/nhess-2019-304
Preprint. Discussion started: 15 October 2019

Author contributions. JE, MR, RM, AC and FV developed the experimental design; whilst JE, JF and JG data curation, fieldworking and figure elaboration. MT carried out the meteorological analysis. BN and FV performed the hydraulic modelling. RM and XP developed the hydrological model code and performed the simulations. MR completed the damage assessment and AC the sediment connectivity and geomorphic change detection. Resources and funding acquisition were supervised by JE and MR. JE prepared the manuscript with contributions from all co-authors.

Acknowledgements

This work was supported by the Spanish Ministry of Science, Innovation and Universities, the Spanish Agency of Research (AEI) and the European Regional Development Funds (ERDF) through the project CGL2017-88200-R "Functional hydrological and sediment connectivity at Mediterranean catchments: global change scenarios –MEDhyCON2". Josep Fortesa has a contract funded by the Vice-presidency and Ministry of Innovation, Research and Tourism of the Autonomous Government of the Balearic Islands (FPI/2048/2017). The contribution of Miquel Tomàs-Burguera was supported by the project CGL2017-83866-C3-3-R also funded by AEI. Julián García-Comendador is in receipt of a pre-doctoral contract (FPU15/05239) funded by the Spanish Ministry of Education and Culture. Meteorological data were facilitated by the Spanish Meteorological Agency (AEMET). We would like to thank BalearsMeteo for providing subhourly rainfall data of the event. Authors want to thank Xurxo Gago, Carlos J. Oliveros, José A. López-Tarazón and Hassan Ouakhir for their assistance during fieldwork. Finally, we want to pay tribute to all the professionals and volunteers who worked determinedly in the tasks of victim's rescue.

References

Adamovic, M., Branger, F., Braud, I. and Kralisch, S.: Development of a data-driven semi-distributed hydrological model for regional scale catchments prone to Mediterranean flash floods, J. Hydrol., 541, 173–189, doi:10.1016/j.jhydrol.2016.03.032, 2016.

Agisoft Lens: Agisoft PhotoScan User Manual. Professional Edition, Version 1.4. [online] Available from: https://www.agisoft.com/pdf/photoscan-pro_1_4_en.pdf (Accessed 12 September 2019), 2018.

Álvaro, M., Del Olmo, P. and Anglada, E.: Mapa Geológico de España, 1991.

Amponsah, W., Marchi, L., Zoccatelli, D., Boni, G., Cavalli, M., Comiti, F., Crema, S., Lucía, A., Marra, F. and Borga, M.: Hydrometeorological Characterization of a Flash Flood Associated with Major Geomorphic Effects: Assessment of Peak Discharge Uncertainties and Analysis of the Runoff Response, J. Hydrometeorol., 17(12), 3063–3077, doi:10.1175/JHM-D-16-0081.1, 2016.

Amponsah, W., Ayral, P.-A., Boudevillain, B., Bouvier, C., Braud, I., Brunet, P., Delrieu, G., Didon-Lescot, J.-F., Gaume, E., Lebouc, L., Marchi, L., Marra, F., Morin, E., Nord, G., Payrastre, O., Zoccatelli, D. and Borga, M.: Integrated high-resolution dataset of high-intensity European and Mediterranean flash floods, Earth Syst. Sci. Data, 10(4), 1783–1794, doi:10.5194/essd-10-1783-2018, 2018.

https://doi.org/10.5194/nhess-2019-304
Preprint. Discussion started: 15 October 2019

Artinyan, E., Vincendon, B., Kroumova, K., Nedkov, N., Tsarev, P., Balabanova, S. and Koshinchanov, G.: Flood forecasting and alert system for Arda River basin, J. Hydrol., 541, 457–470, doi:10.1016/j.jhydrol.2016.02.059, 2016.

Barbosa, S., Silva, Á. and Narciso, P.: Analysis of the 1 November 2015 heavy rainfall episode in Algarve by using weather radar and rain gauge data, Nat. Hazards, 93(S1), 61–76, doi:10.1007/s11069-017-3065-2, 2018.

Barredo, J. I.: Major flood disasters in Europe: 1950–2005, Nat. Hazards, 42(1), 125–148, doi:10.1007/s11069-006-9065-2, 2007.

BOE: Boletín Oficial del Estado (BOE Nº 283) (23/11/2018). Decreto-ley 2/2018, de 18 de octubre, por el que se establecen ayudas y otras medidas urgentes para reparar las pérdidas y los daños producidos por las lluvias intensas y las inundaciones del día 9 de , Spain. [online] Available from: https://www.boe.es/boe/dias/2018/11/23/pdfs/BOE-A-2018-15970.pdf, 2018.

Borga, M., Boscolo, P., Zanon, F. and Sangati, M.: Hydrometeorological Analysis of the 29 August 2003 Flash Flood in the Eastern Italian Alps, J. Hydrometeorol., 8(5), 1049–1067, doi:10.1175/jhm593.1, 2007.

Borga, M., Gaume, E., Creutin, J. D. and Marchi, L.: Surveying flash floods: gauging the ungauged extremes, Hydrol. Process., 22(18), 3883–3885, doi:10.1002/hyp.7111, 2008.

Borselli, L., Cassi, P. and Torri, D.: Prolegomena to sediment and flow connectivity in the landscape: A GIS and field numerical assessment, CATENA, 75(3), 268–277, doi:10.1016/j.catena.2008.07.006, 2008.

Braud, I., Ayral, P.-A., Bouvier, C., Branger, F., Delrieu, G., Le Coz, J., Nord, G., Vandervaere, J.-P., Anquetin, S., Adamovic, M., Andrieu, J., Batiot, C., Boudevillain, B., Brunet, P., Carreau, J., Confoland, A., Didon-Lescot, J.-F., Domergue, J.-M., Douvinet, J., Dramais, G., Freydier, R., Gérard, S., Huza, J., Leblois, E., Le Bourgeois, O., Le Boursicaud, R., Marchand, P., Martin, P., Nottale, L., Patris, N., Renard, B., Seidel, J.-L., Taupin, J.-D., Vannier, O. and Wijbrans, A.: Multi-scale hydrometeorological observation and modelling for flash flood understanding, Hydrol. Earth Syst. Sci, 18, 3733–3761, doi:10.5194/hess-18-3733-2014, 2014.

Cavalli, M., Trevisani, S., Comiti, F. and Marchi, L.: Geomorphometric assessment of spatial sediment connectivity in small Alpine catchments, Geomorphology, 188, 31–41, doi:10.1016/j.geomorph.2012.05.007, 2013.

CCS: Estudio Siniestralidades 2018. Inundación extraordinaria Mallorca: Sant Llorenç des Cardassar. Consorcio de Compensación de Seguros. Ministerio de Economía y Empresa. Gobierno de España, [online] Available from: https://www.consorseguros.es/web/inicio, 2018.

Chapon, B., Delrieu, G., Gosset, M. and Boudevillain, B.: Variability of rain drop size distribution and its effect on the Z–R relationship: A case study for intense Mediterranean rainfall, Atmos. Res., 87(1), 52–65, doi:10.1016/j.atmosres.2007.07.003, 2008.

Copernicus Emergency Management Service: [EMSR323] Flood in Balearic Island, Spain. [online] Available from: https://emergency.copernicus.eu/mapping/list-of-components/EMSR323, 2018.

Copernicus Emergency Management Service: Directorate Space, Security and Migration, European Commission Joint Research Centre, [online] Available from: https://emergency.copernicus.eu/ (Accessed 14 August 2019), 2019.

Corine Land Cover: Copernicus Land Monitoring Service, [online] Available from: https://land.copernicus.eu/pan-

https://doi.org/10.5194/nhess-2019-304
Preprint. Discussion started: 15 October 2019

european/corine-land-cover/clc2018, 2018.

Crema, S. and Cavalli, M.: SedInConnect: a stand-alone, free and open source tool for the assessment of sediment connectivity, Comput. Geosci., 111, 39–45, doi:10.1016/j.cageo.2017.10.009, 2018.

Defossez, S. and Leone, F.: Assessing Vulnerability to Flooding: Progress and Limitations, Floods, 241–257, doi:10.1016/B978-1-78548-268-7.50014-6, 2017.

Duo, E., Trembanis, A. C., Dohner, S., Grottoli, E. and Ciavola, P.: Local-scale post-event assessments with GPS and UAV-based quick-response surveys: a pilot case from the Emilia–Romagna (Italy) coast, Nat. Hazards Earth Syst. Sci., 18(11), 2969–2989, doi:10.5194/nhess-18-2969-2018, 2018.

ESRI: Arc Hydro Tools, [online] Available from: https://www.esri.com/en-us/home, 2019.

Estrany, J. and Grimalt, M.: Catchment controls and human disturbances on the geomorphology of small Mediterranean estuarine systems, Estuar. Coast. Shelf Sci., 150, 230–241, doi:10.1016/j.ecss.2014.03.021, 2014.

Estrany, J., Garcia, C. and Batalla, R. J.: Groundwater control on the suspended sediment load in the Na Borges River, Mallorca, Spain, Geomorphology, 106(3–4), 292–303, doi:10.1016/J.GEOMORPH.2008.11.008, 2009.

Estrany, J., Ruiz, M., Calsamiglia, A., Carriquí, M., García-Comendador, J., Nadal, M., Fortesa, J., López-Tarazón, J. A., Medrano, H. and Gago, J.: Sediment connectivity linked to vegetation using UAVs: High-resolution imagery for ecosystem management, Sci. Total Environ., 671, 1192–1205, doi:10.1016/j.scitotenv.2019.03.399, 2019.

Fortesa, J., García-Comendador, J., Calsamiglia, A., López-Tarazón, J. A., Latron, J., Alorda, B. and Estrany, J.: Comparison of stage/discharge rating curves derived from different recording systems: Consequences for streamflow data and water management in a Mediterranean island, Sci. Total Environ., 665, 968–981, doi:10.1016/j.scitotenv.2019.02.158, 2019.

García-Hernández, J., Jordan, J., Dubois, J., Boillat, J. and Schleiss, A.: Routing System II: Flow modelling in hydraulic systems., Communication, 32, 1661–1179, 2007.

Gaume, E., Bain, V., Bernardara, P., Newinger, O., Barbuc, M., Bateman, A., Blaškovičová, L., Blöschl, G., Borga, M., Dumitrescu, A., Daliakopoulos, I., Garcia, J., Irimescu, A., Kohnova, S., Koutroulis, A., Marchi, L., Matreata, S., Medina, V., Preciso, E., Sempere-Torres, D., Stancalie, G., Szolgay, J., Tsanis, I., Velasco, D. and Viglione, A.: A compilation of data on European flash floods, J. Hydrol., 367(1–2), 70–78, doi:10.1016/J.JHYDROL.2008.12.028, 2009.

Gaume, E., Borga, M., Llasat, M. C., Maouche, S., Lang, M. and Diakakis, M.: Mediterranean extreme floods and flash floods, in The Mediterranean Region under Climate Change. A Scientific Update, edited by Allenvi, pp. 133–144. [online] Available from: https://hal.archives-ouvertes.fr/hal-01465740v2/document, 2016.

Georgakakos, K. P.: On the Design of National, Real-Time Warning Systems with Capability for Site-Specific, Flash-Flood Forecasts, Bull. Am. Meteorol. Soc., 67(10), 1233–1239, doi:10.1175/1520-0477(1986)067<1233:OTDONR>2.0.CO;2, 1986.

GOIB: Mapas de peligrosidad y riesgo de inundación en la demarcación hidrográfica de Baleares. Conselleria de Medi Ambient, Agricultura i Pesca-Direcció General de Recursos Hídrics. [online] Available from: https://www.caib.es/sites/aigua/es/plan_de_gestion_del_riesgo_de_inundacion_de_la_demarcacion_hidrografica_de_las_isla

https://doi.org/10.5194/nhess-2019-304
Preprint. Discussion started: 15 October 2019

s_baleares/, 2016.

GOIB: Boletín Oficial de las Islas Baleares (BOIB Nº 130) (18/10/2018). Decreto-ley 2/2018, de 18 de octubre, por el que se establecen ayudas y otras medidas urgentes para reparar las pérdidas y los daños producidos por las lluvias intensas y las inundaciones d. [online] Available from: http://www.caib.es/eboibfront/pdf/ca/2018/130/101958, 2018.

Gourley, J. J., Giangrande, S. E., Hong, Y., Flamig, Z. L., Schuur, T. and Vrugt, J. A.: Impacts of Polarimetric Radar Observations on Hydrologic Simulation, J. Hydrometeorol., 11(3), 781–796, doi:10.1175/2010JHM1218.1, 2010.

Guijarro, J. A.: Contribución a la Bioclimatología de Baleares, Universitat de les Illes Balears., 1986.

Hardy, J., Gourley, J., Kirstetter, P., Hong, Y., Kong, F. and Flamig, Z.: A method for probabilistic flash flood forecasting, J. Hydrol., 541, 480–494 [online] Available from: https://www.sciencedirect.com/science/article/pii/S0022169416301883 (Accessed 11 September 2019), 2016.

Harrison, D., Driscoll, S. and Kitchen, M.: Improving precipitation estimates from weather radar using quality control and correction techniques, Meteorol. Appl., 7(2), 135–144, doi:https://doi.org/10.1017/S1350482700001468, 2000.

Jordan, F.: Modèle de prévision et de gestion des crues-optimisation des opérations des aménagements hydroélectriques à accumulation pour la réduction des débits de crue, Laboratory of Hydraulic Construction, Ecole Polytechnique Fédérale de Lausanne, Lausanne., 2007.

Kalantari, Z., Cavalli, M., Cantone, C., Crema, S. and Destouni, G.: Flood probability quantification for road infrastructure: Data-driven spatial-statistical approach and case study applications, Sci. Total Environ., 581–582, 386–398, doi:10.1016/J.SCITOTENV.2016.12.147, 2017.

Laudan, J., Rözer, V., Sieg, T., Vogel, K. and Thieken, A. H.: Damage assessment in Braunsbach 2016: data collection and analysis for an improved understanding of damaging processes during flash floods, Nat. Hazards Earth Syst. Sci., 17(12), 2163–2179, doi:10.5194/nhess-17-2163-2017, 2017.

Li, Z., Xu, X., Zhu, J., Xu, C. and Wang, K.: Effects of lithology and geomorphology on sediment yield in karst mountainous catchments, Geomorphology, 343, 119–128, doi:10.1016/j.geomorph.2019.07.001, 2019.

Llasat, M. C., Llasat-Botija, M., Petrucci, O., Pasqua, A. A., Rosselló, J., Vinet, F. and Boissier, L.: Towards a database on societal impact of Mediterranean floods within the framework of the HYMEX project, Nat. Hazards Earth Syst. Sci., 13(5), 1337–1350, doi:10.5194/nhess-13-1337-2013, 2013.

Lowe, D.: Distinctive Image Features from Scale-Invariant Keypoints, Vancouver. [online] Available from: https://robo.fish/wiki/images/5/58/Image_Features_From_Scale_Invariant_Keypoints_Lowe_2004.pdf (Accessed 11 September 2019), 2004.

Marchi, L., Borga, M., Preciso, E. and Gaume, E.: Characterisation of selected extreme flash floods in Europe and implications for flood risk management, J. Hydrol., 394(1–2), 118–133, doi:10.1016/j.jhydrol.2010.07.017, 2010.

Marshall, J. S. and Palmer, W. M. K.: The distribution of raindrops with size, J. Meteorol., 5(4), 165–166, doi:10.1175/1520-0469(1948)005<0165:TDORWS>2.0.CO;2, 1948.

Miao, Q., Yang, D., Yang, H. and Li, Z.: Establishing a rainfall threshold for flash flood warnings in China's mountainous

https://doi.org/10.5194/nhess-2019-304
Preprint. Discussion started: 15 October 2019

areas based on a distributed hydrological model, J. Hydrol., 541, 371–386, doi:10.1016/j.jhydrol.2016.04.054, 2016.

Nguyen, P., Thorstensen, A., Sorooshian, S., Hsu, K., AghaKouchak, A., Sanders, B., Koren, V., Cui, Z. and Smith, M.: A high resolution coupled hydrologic–hydraulic model (HiResFlood-UCI) for flash flood modeling, J. Hydrol., 541, 401–420, doi:10.1016/j.jhydrol.2015.10.047, 2016.

Petrus, J. M., Ruiz, M. and Estrany, J.: Interactions between Geomorphology and Urban Evolution Since Neolithic Times in a Mediterranean City, Urban Geomorphol., 9–35, doi:10.1016/B978-0-12-811951-8.00002-3, 2018.

Piaggesi, D., Sund, K. J. and Castelnovo, W.: Global strategy and practice of e-governance : examples from around the world, Information Science Reference. [online] Available from: https://books.google.es/books?id=ncEEYjRNSmcC&pg=PA282&lpg=PA282&dq=cadastre+info+as+damage+assessment&source=bl&ots=ik0CeebQ2L&sig=ACfU3U1Hgw3A2tPoHbSfk6hXtmmloCIi-w&hl=ca&sa=X&ved=2ahUKEwiHtafnqbzkAhWzAWMBHWUEBuwQ6AEwDnoECAgQAQ#v=onepage&q=cadastre info as damage assessment&f=false (Accessed 9 September 2019), 2011.

Plank, S.: Rapid Damage Assessment by Means of Multi-Temporal SAR — A Comprehensive Review and Outlook to Sentinel-1, Remote Sens., 6(6), 4870–4906, doi:10.3390/rs6064870, 2014.

PNOA: Plan Nacional de Ortofotografía Aérea. Instituto Geográfico Nacional, Ministerio de Fomento, Gobierno de España, [online] Available from: https://pnoa.ign.es/productos_lidar, 2015.

Poesen, J. and Lavee, H.: Rock fragments in top soils: significance and processes, Catena, 23(1–2), 1–28 [online] Available from: https://www.sciencedirect.com/science/article/pii/0341816294900507 (Accessed 11 September 2019), 1994.

Pol, J.: Informe INUNBAL Llevant Mallorca 2018. ISO 271/2018, Marratxí., 2019.

Pons Esteva, A.: Evolució dels usos del sòl a les illes Balears. 1956- 2000, Territoris, (4), 129–145, 2003.

Schaefli, B., Hingray, B., Niggli, M. and Musy, A.: A conceptual glacio-hydrological model for high mountainous catchments, Hydrol. Earth Syst. Sci., 9(1), 95–109 [online] Available from: https://hal.archives-ouvertes.fr/hal-00304808/ (Accessed 11 September 2019), 2005.

Schoorl, J. M., Boix Fayos, C., de Meijer, R. J., van der Graaf, E. R. and Veldkamp, A.: The 137Cs technique applied to steep Mediterranean slopes (Part II): landscape evolution and model calibration, CATENA, 57(1), 35–54 [online] Available from: http://www.sciencedirect.com/science/article/B6VCG-4B0SYSG-1/2/3ff40d138582e1585f94703cbd83bd67, 2004.

Segura-Beltrán, F., Sanchis-Ibor, C., Morales-Hernández, M., González-Sanchis, M., Bussi, G. and Ortiz, E.: Using post-flood surveys and geomorphologic mapping to evaluate hydrological and hydraulic models: The flash flood of the Girona River (Spain) in 2007, J. Hydrol., 541, 310–329, doi:10.1016/J.JHYDROL.2016.04.039, 2016.

Shepard, D.: A two-dimensional interpolation function for irregularly-spaced data, in Proceedings of the 1968 23rd ACM national conference, pp. 517–524. [online] Available from: http://citeseerx.ist.psu.edu/viewdoc/download?doi=10.1.1.154.6880&rep=rep1&type=pdf (Accessed 11 September 2019), 1968.

Trevisani, S. and Cavalli, M.: Topography-based flow-directional roughness: potential and challenges, Earth Surf. Dyn.,

https://doi.org/10.5194/nhess-2019-304
Preprint. Discussion started: 15 October 2019

4(2), 343–358, doi:10.5194/esurf-4-343-2016, 2016.

Vannier, O., Anquetin, S. and Braud, I.: Investigating the role of geology in the hydrological response of Mediterranean catchments prone to flash-floods: Regional modelling study and process understanding, J. Hydrol., 541, 158–172, doi:10.1016/J.JHYDROL.2016.04.001, 2016.

Versini, P.-A., Velasco, M., Cabello, A. and Sempere-Torres, D.: Hydrological impact of forest fires and climate change in a Mediterranean basin, Nat. Hazards, 66(2), 609–628, doi:10.1007/s11069-012-0503-z, 2013.

Wainwright, J. and Thornes, J. B.: Environmental issues in the Mediterranean. Processes and perspectives from the past and present, 1st ed., edited by Routledge, Routledge, London., 2004.

Westoby, M. J., Brasington, J., Glasser, N. F., Hambrey, M. J. and Reynolds, J. M.: 'Structure-from-Motion' photogrammetry: A low-cost, effective tool for geoscience applications, Geomorphology, 179, 300–314, doi:10.1016/j.geomorph.2012.08.021, 2012.

YACU: Estudio de caracterización del régimen extremo de precipitaciones en la isla de Mallorca, Junta d'Aigües de les Illes Balears, Palma de Mallorca., 2003.

https://doi.org/10.5194/nhess-2019-304
Preprint. Discussion started: 15 October 2019

Natural Hazards and Earth System Sciences
Discussions

Tables and captions

(a)

Event rainfall duration (h)	Time of maximum rainfall	Centroid storm	Average radar rainfall (mm)	IP_{max} average radar (mm h^{-1})	IP_{max} radar (mm h^{-1})	IP average radar (mm h^{-1})
10	09/10/18 18:00	09/10/2018 17:00	246	46	77	24

(b)

Runoff (mm)	Runoff ratio	Event duration (h)	Q_{max} (m^3 s^{-1})	Time Q_{max}	T centroid storm-T Q_{max} (h)	$Q_{average}$ (m^3 s^{-1})	Unit peak discharge (m^3 s^{-1} km^2)	Reduced Unit peak discharge (m^3 s^{-1} km^2)
86	0.36	12	442	09/10/18 19:15	0.25	26	19	67

Table 1 (a) Rainfall and (b) runoff variables of the flash flood at the Begura de Saumà River catchment estimated from the continuous water stage monitoring at the MEDhyCON hydrometric station located in the village of Sant Llorenç des Cardassar.

People and goods		**Buildings**	
Death toll	13	Emergency interventions into the structure	52
Slightly injured	4	Demolitions	3
Initial missing persons	74	Affected buildings	> 1000
Infrastructure damages		**Movable properties**	
Cut roads	4 main roads	Motor vehicles	426
Affected roads	22 road sections		
Bridges	8 with structural damages	**Actions undertaken**	
Public hydraulic domain	High affection	Rubble removal	7,000 tones
Drinking and wasting water network	Several damages	Human Emergency resources mobilized	> 200
Telecom infrastructures	Severe damages		
Electricity network	Undetermined severe damages 8355 affected users	Rescue assistance	342 persons

Table 2 Damage summary and emergency actions of the 9th October 2018 violent flash-flood carried out in the Llevant County of Mallorca. Source: Pol (2019).

https://doi.org/10.5194/nhess-2019-304
Preprint. Discussion started: 15 October 2019

Natural Hazards and Earth System Sciences
Discussions

Damage level	Flood risk cartographies						Copernicus Emergency Management System		Total
	10 years	*%*	*100 years*	*%*	*500 years*	*%*	*Affected area*	*%*	
COLLAPSED	5	50	8	80	9	90	10	100	10
DAMAGED & HABITABLE	52	20	107	41	141	54	225	86	261
DAMAGED & NO HABITABLE	15	41	26	70	31	84	36	97	37
DAMAGED PLOT	6	35	9	53	9	53	13	76	17
DAMAGED & RESTRINGED USE	19	28	39	58	47	70	63	94	67
TOTAL	97	25	189	48	237	60	347	89	392

Table 3 Damaged buildings in the village of Sant Llorenç des Cardassar caused by the violent flash-flood in 9th October 2018 and encompassed in the official flood risk maps for 10, 100 and 500 years recurrence period.

840

https://doi.org/10.5194/nhess-2019-304
Preprint. Discussion started: 15 October 2019

Natural Hazards and Earth System Sciences
Discussions

Figures and captions

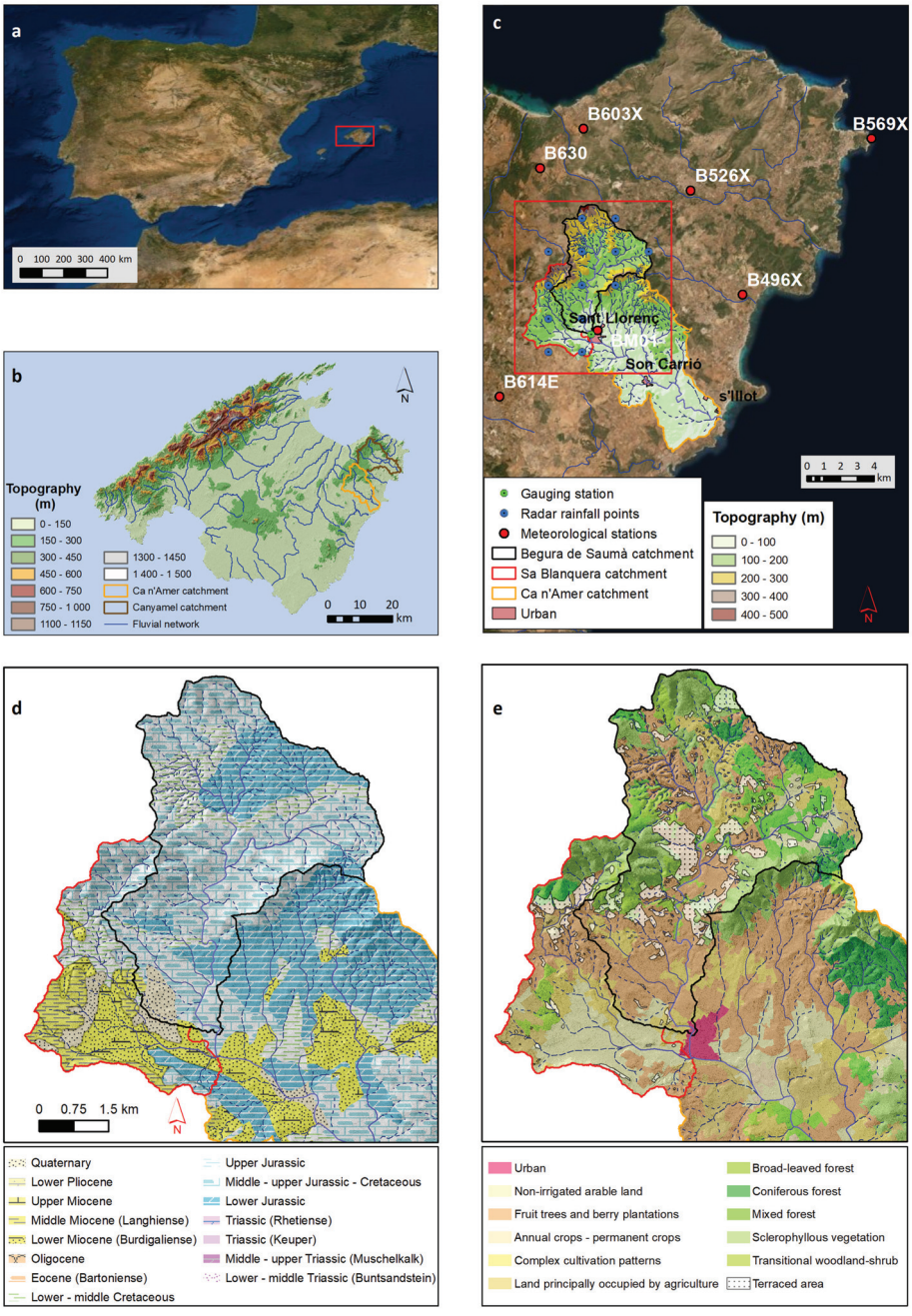

Figure 1 Main characteristics of affected basins during the 9th October 2018 flash-flood. (a) Location of Mallorca in western Mediterranean. (b) Topography and fluvial network of Mallorca Island with the location of the affected main basins: Canyamel and Ca n'Amer rivers. (c) Blanquera and Begura de Saumà headwater river catchments within the Ca n'Amer River locating rainfall and hydrometric stations, and radar rainfall points derived from a regular mesh of 1x1 km. Source: https://opendata.aemet.es. Background: aerial photography and DEM data (PNOA, 2015). (d) Lithology of both Blanquera and Begura de Saumà catchments. (e) Land uses and terraced areas for the same headwater catchments. Source: Corine Land Cover (2018).

https://doi.org/10.5194/nhess-2019-304
Preprint. Discussion started: 15 October 2019

Natural Hazards and Earth System Sciences
Discussions
Open Access
EGU

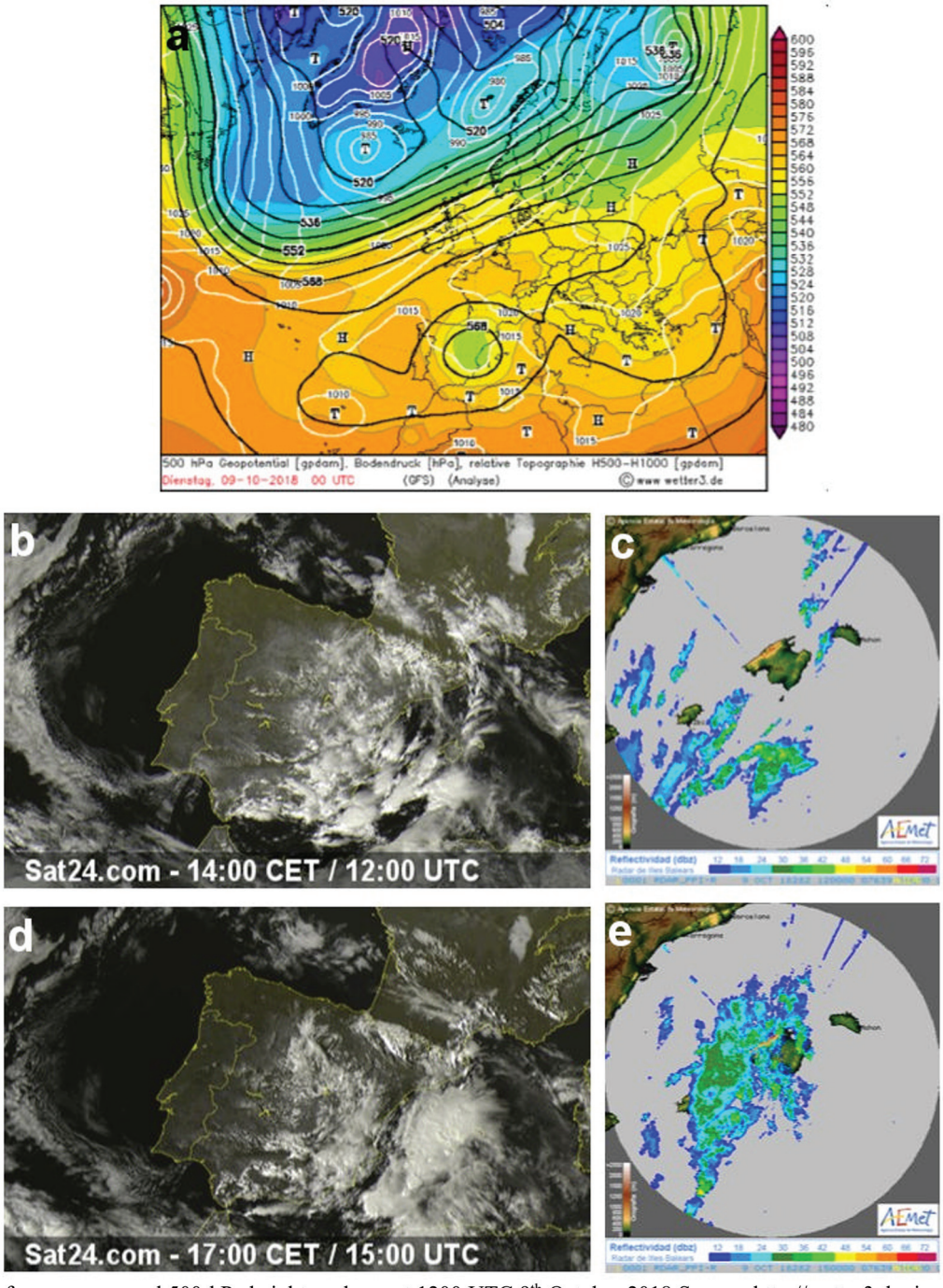

Figure 2 (a) Surface pressure and 500-hPa height analyses at 1200 UTC 9th October 2018 Source: http://wetter3.de; i.e. , at the beginning of the precipitation event. Satellite image at (b) 12.00UTC and (d) 15.00UTC Source: http://www.sat24.com. EUMETSAT and radar images at the same hours (c and e) Source: http://www.aemet.es.

https://doi.org/10.5194/nhess-2019-304
Preprint. Discussion started: 15 October 2019

Natural Hazards and Earth System Sciences
Discussions
Open Access
EGU

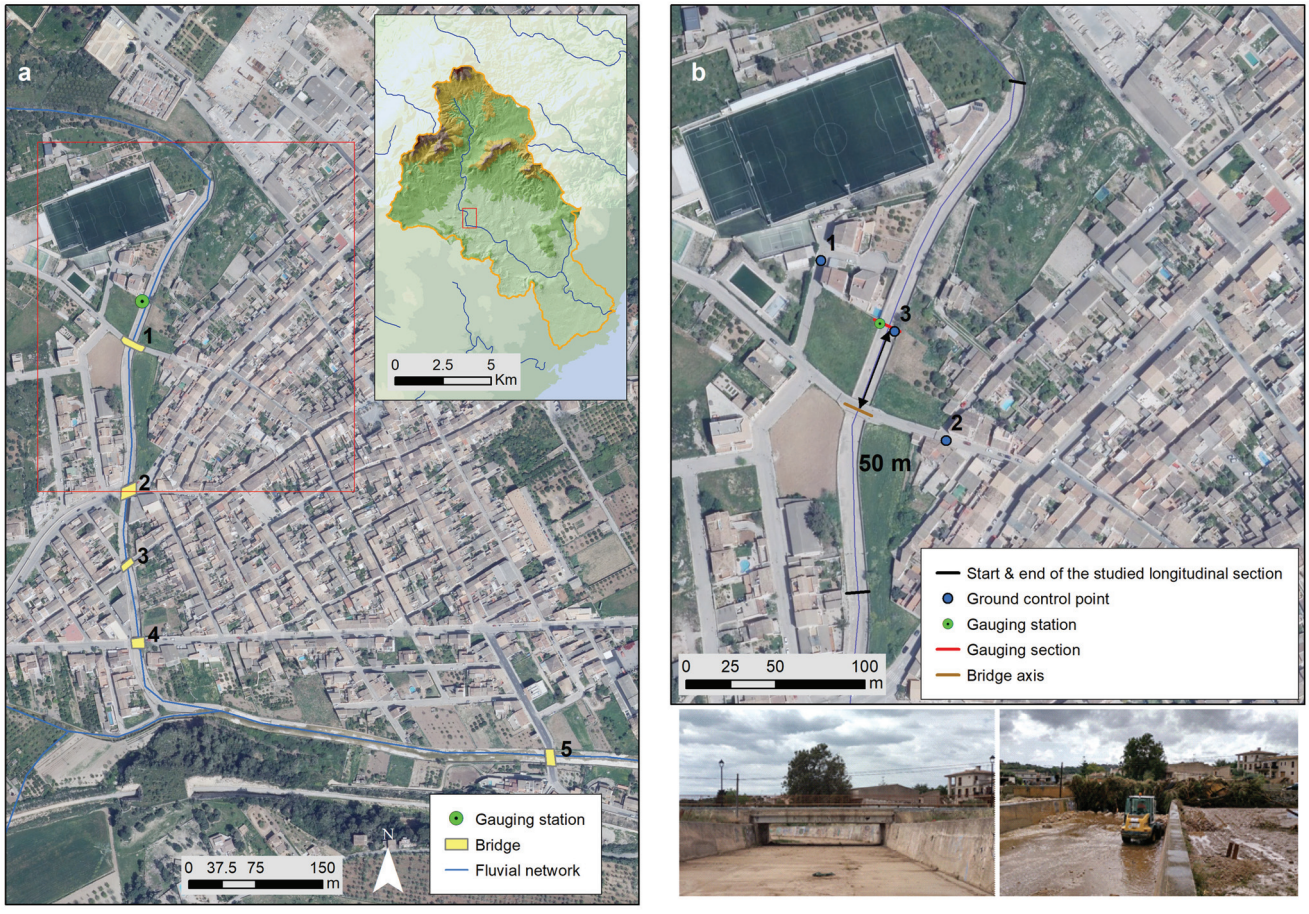

Figure 3 (a) Aerial view of the Begura de Saumà River of concrete channelization that crosses Sant Llorenç des Cardassar village and the location of bridges. (b) Detailed aerial view of the very beginning of this concrete channelization where the hydrometric station is located. The photographs show a view of the Bridge 1 from the hydrometric station when (the right picture) was installed the digital equipment, 10th June 2015 and (the left one) few hours after the flash flood, the 10th October 2018. Background: aerial photography and DEM data (PNOA, 2015).

https://doi.org/10.5194/nhess-2019-304
Preprint. Discussion started: 15 October 2019

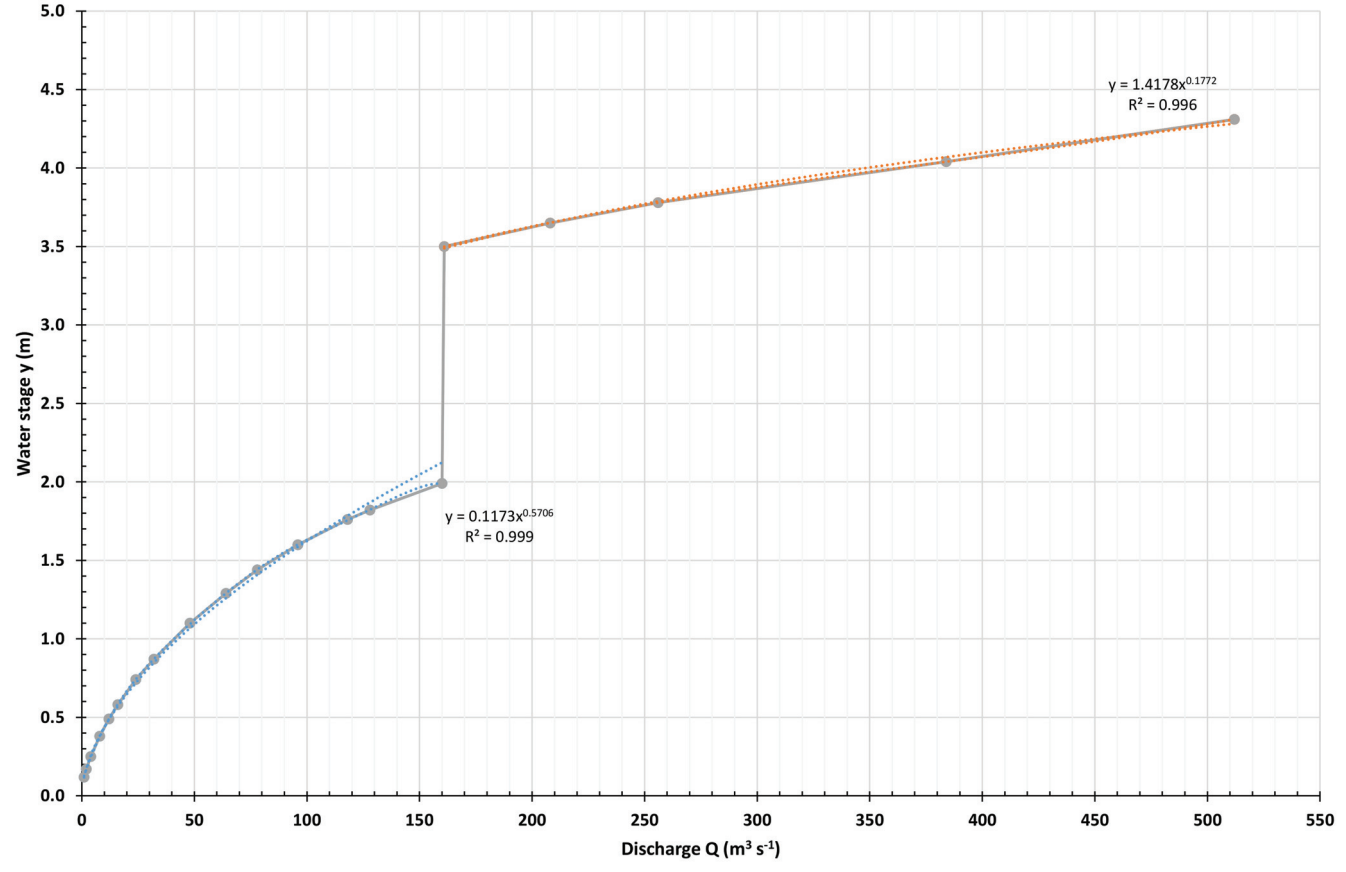

Figure 4 Stage-discharge rating curve performed by means of two-dimensional hydraulic modelling with two differentiated sections in according to the influence of the Bridge 1 (see Figure 3a) and its potential obstruction.

https://doi.org/10.5194/nhess-2019-304
Preprint. Discussion started: 15 October 2019

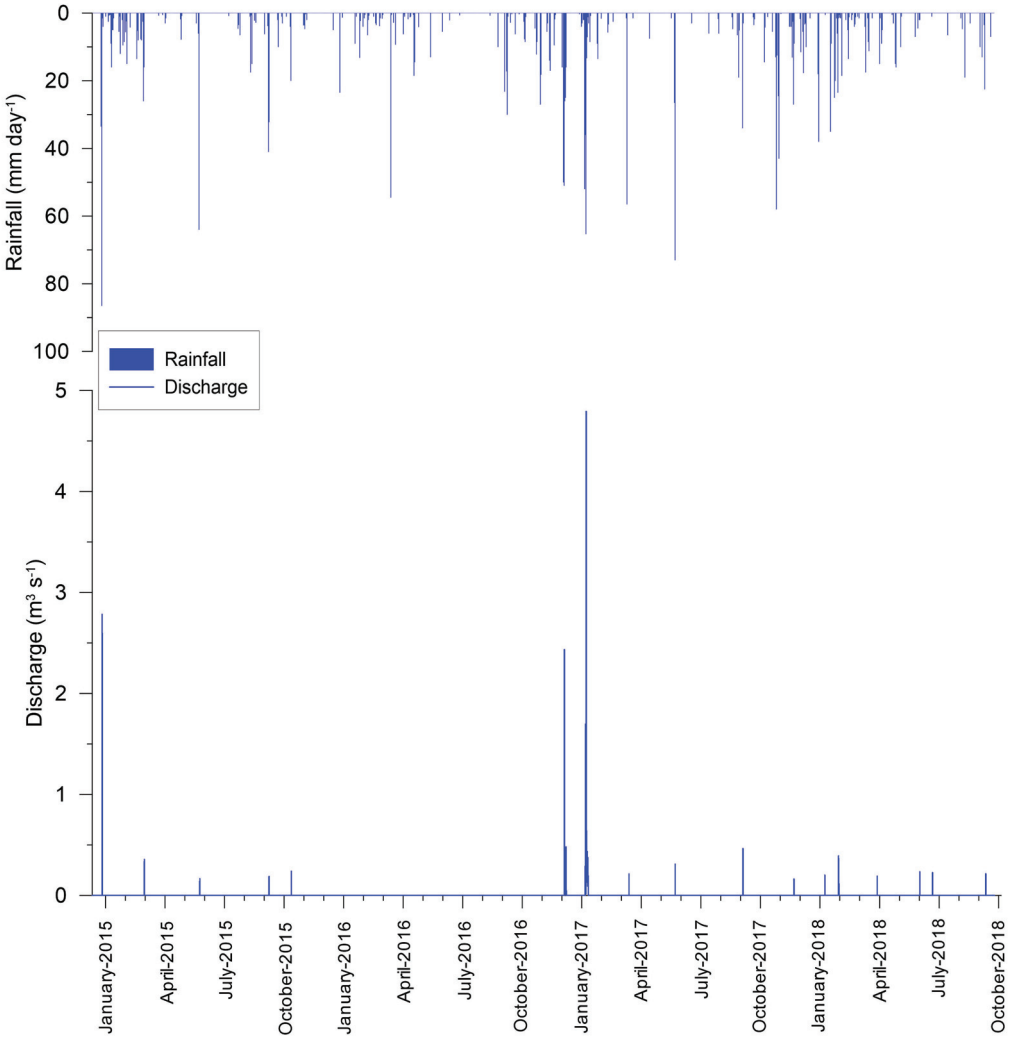

Hydrological year	Rainfall (mm)	Runoff (mm)	Qmax ($m^3 s^{-1}$)	Qavg ($m^3 s^{-1}$)
2014-15	823	2.0	2.8	0.002
2015-16	363	0.1	0.2	0.000
2016-17	825	12.9	4.8	0.009
2017-18	763	0.8	0.4	0.001
2018-19 (until April)	500	91.8	442.0	0.118
Average study period (2014-2018)	655 ± 211	21.5	---	0.026 ± 0.1
Average long term (1968-2018)	652 ± 176	---	---	---

Figure 5 Discharge at 15-min interval measured in the MEDhyCON hydrometric station located at the beginning of concrete channelization of the Begura de Saumà River in Sant Llorenç des Cardassar. Likewise, daily rainfall measured at the AEMET- B630 Ses Pastores during the monitored period (10th January 2015-30th September 2018), previous to the catastrophic flash flood of 9th October 2018. Bottom set table: Rainfall, runoff and peak discharge for hydrological years during study period. Rainfall data is from AEMET-B630 Ses Pastores, located 10.5 km from the Begura de Saumà catchment outlet and representative of rainfall dynamics of the Llevant Ranges headwater parts.

https://doi.org/10.5194/nhess-2019-304
Preprint. Discussion started: 15 October 2019

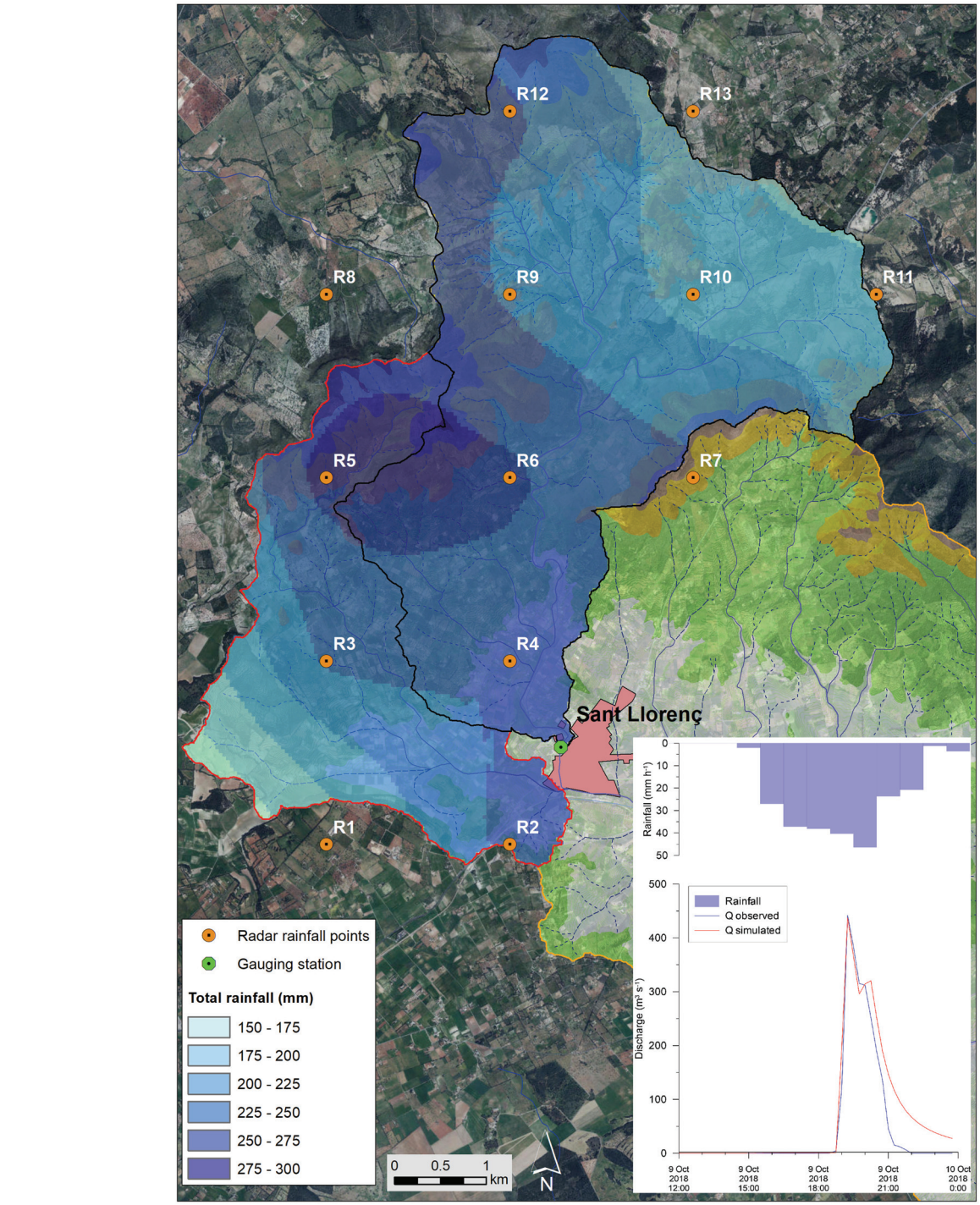

Figure 6 Map of isohyets of the rain storm occurred 9th October 2018 in the two headwater catchments of the Ca n'Amer River; i.e., Blanquera and Begura de Saumà rivers. Source: 10-minute radar images obtained from the web https://opendata.aemet.es/. The inset figure illustrates the observed discharge measured at the MEDhyCON hydrometric station as well as the result of the rainfall-runoff simulation using a modified version of the GR3 model. Background: aerial photography and DEM data (PNOA, 2015).

https://doi.org/10.5194/nhess-2019-304
Preprint. Discussion started: 15 October 2019

Natural Hazards and Earth System Sciences
Discussions

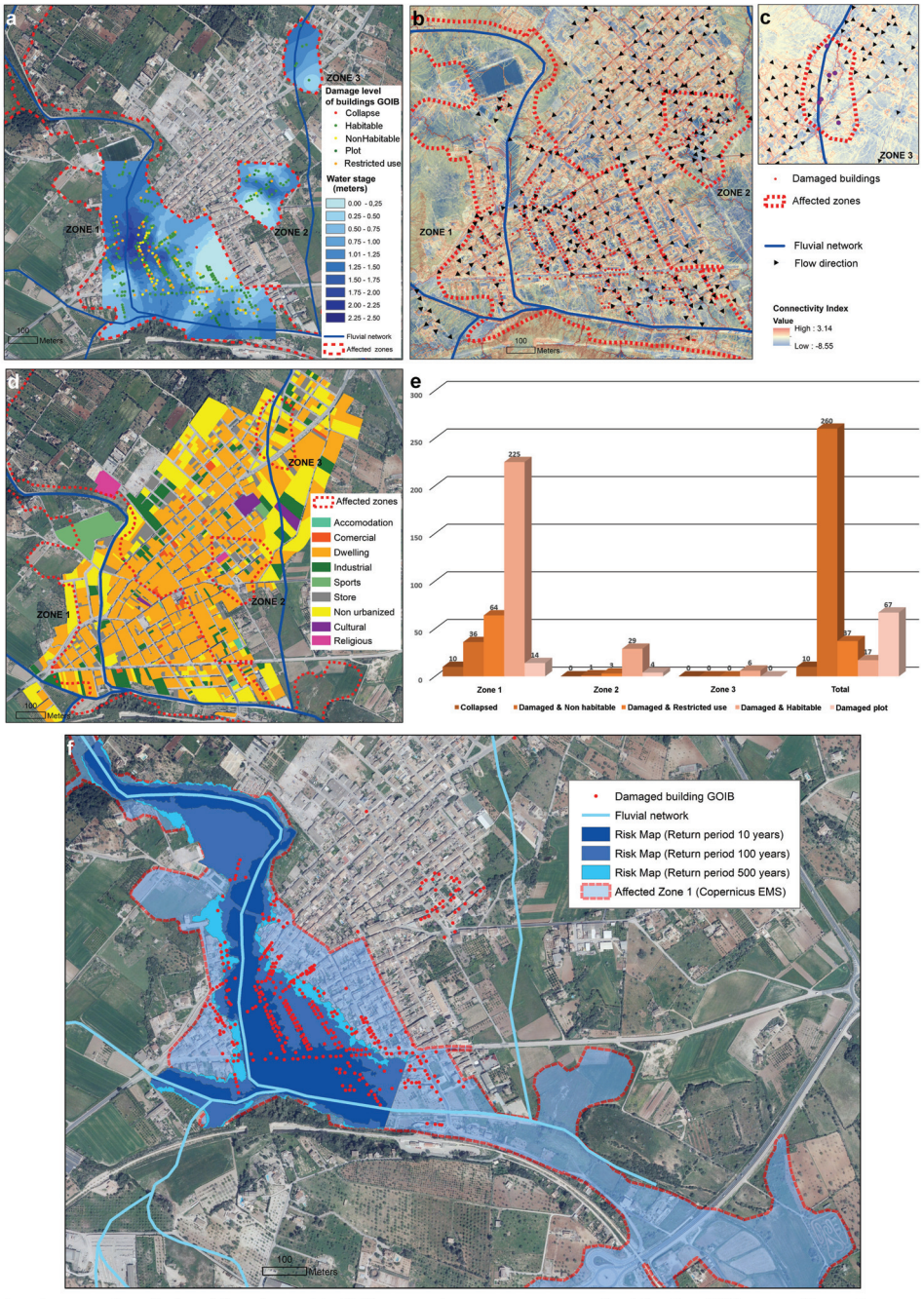

Figure 7 (a) Map of the damage level classification of buildings and water stage reached in the different affected zones at Sant Llorenç des Cardassar according to Balearic Islands Autonomous Government in comparison with the flood delimitation carried out by Copernicus EMS. Flow direction and hydrological connectivity in the affected zones (b) 1 and 2, as well as (c) 3 in the Sant Llorenç des Cardassar urban network. (d) Economic activities at building scale in the urban area of Sant Llorenç des Cardassar and the delimitation of affected zones by the flash-flood. (e) Damage level classification of buildings in the different affected zones at Sant Llorenç des Cardassar. (f) Damage level of the buildings and plots by zones. (f) Official flood risk maps and flood delimitation by Copernicus EMS at the Sant Llorenç des Cardassar village with the location of affected buildings by the flash-flood occurred 9th October 2018. Background: aerial photography (PNOA, 2015). In Fig. 7d, the source of land uses at urban plot scale is the General Directorate for the Cadastre (http://www.sedecatastro.gob.es/).

https://doi.org/10.5194/nhess-2019-304
Preprint. Discussion started: 15 October 2019

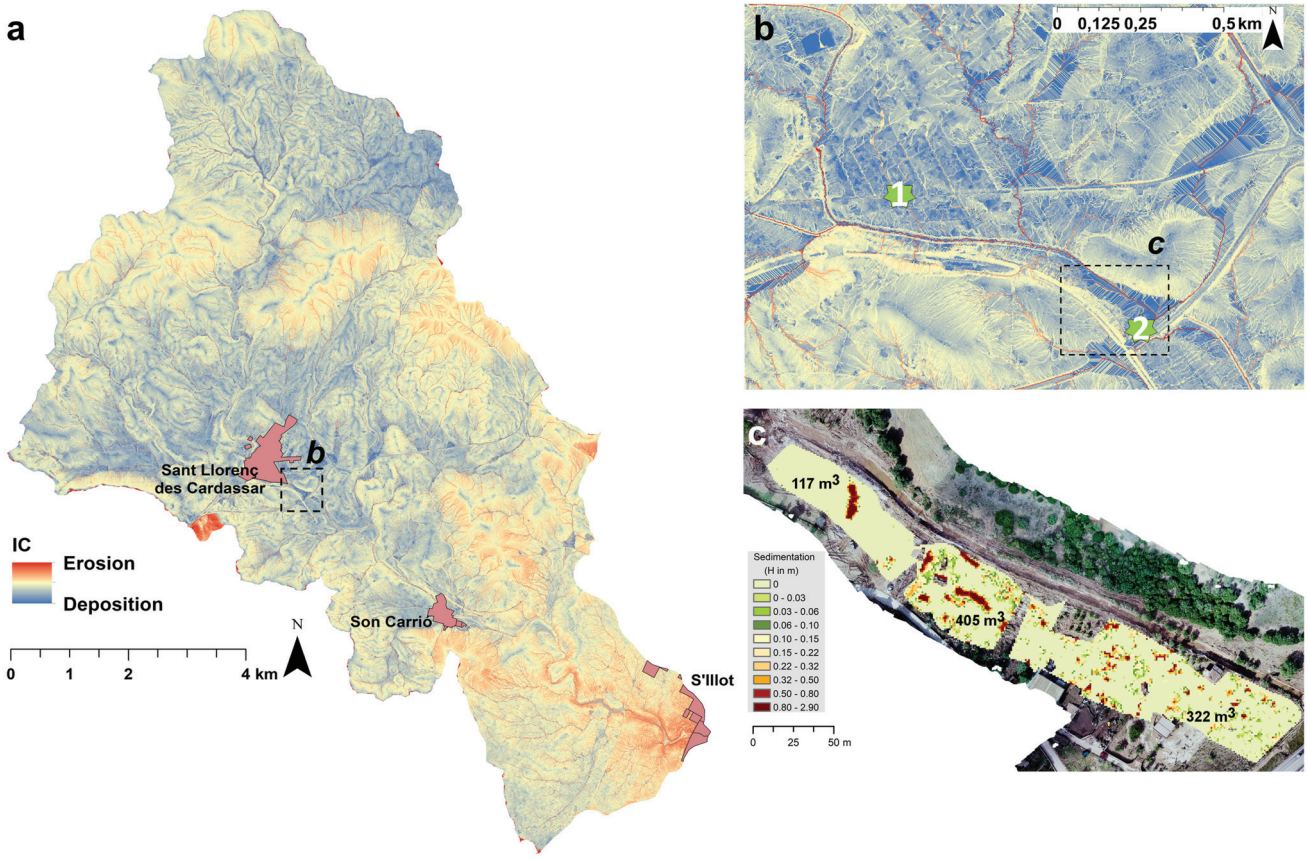

Figure 8 Spatial patterns of hydrological and sediment connectivity (deposition zones in blue colours) (a) in the Ca n'Amer River basin, (b) in the south-east part of Sant Llorenç des Cardassar with numbers indicate (1) the point where the missing person was last seen and (2) where this person was found with the application of this connectivity index from a digital terrain model (MDT) of 2 m resolution (Instituto Geográfico Nacional, 2014). (c) Overbank sedimentation estimated after the flash-flood from a DEM performed with SfM from a UAV flight (15th October 2018) in relation to the ground points of the 2014 LiDAR data. Back ground aerial orthophotography of ca. 2 cm resolution obtained also from the drone images. Numbers indicate the total volume of deposited sediments in the three measured areas.